

Energy Norm Based A Posteriori Error Estimation for Boundary Element Methods in Two Dimensions

Christoph Erath, Samuel Ferraz-Leite, Stefan Funken und Dirk
Praetorius

Preprint Series: 2007-12



Fakultät für Mathematik und Wirtschaftswissenschaften
UNIVERSITÄT ULM

ENERGY NORM BASED A POSTERIORI ERROR ESTIMATION FOR BOUNDARY ELEMENT METHODS IN TWO DIMENSIONS

C. ERATH, S. FERRAZ-LEITE, S. FUNKEN, AND D. PRAETORIUS

ABSTRACT. A posteriori error estimation is an important tool for reliable and efficient Galerkin boundary element computations. We analyze the mathematical relation between the h - $h/2$ -error estimator from [8], the two-level error estimator from [15], and the averaging error estimator from [3]. We essentially show that all of these are equivalent, and we extend the analysis of [15] to cover adaptive mesh-refinement. Therefore, all error estimators give lower bounds for the Galerkin error, whereas upper bounds depend crucially on the saturation assumption. As model example serve first-kind integral equations in 2D with weakly singular integral kernel.

Dedicated to Professor Ernst P. Stephan on the occasion of his 60th birthday

1. INTRODUCTION AND MODEL EXAMPLE

We consider Symm's integral equation

$$(1.1) \quad V\phi = f \quad \text{on } \Gamma$$

for a relatively open subset $\Gamma \subseteq \partial\Omega$ of the boundary of a bounded Lipschitz domain $\Omega \subseteq \mathbb{R}^2$. Here, $V\phi$ denotes the simple-layer potential which reads, e.g., for the Laplace operator

$$(1.2) \quad V\phi(x) = -\frac{1}{2\pi} \int_{\Gamma} \log|x-y|\phi(y) ds_y \quad \text{for } x \in \Gamma,$$

where $\int_{\Gamma} ds$ denotes the integration over the surface piece Γ . Provided $\text{diam}(\Omega) < 1$, the operator $V : \tilde{H}^{-1/2}(\Gamma) \rightarrow H^{1/2}(\Gamma)$ is a symmetric and elliptic isomorphism between the fractional-order Sobolev space $\mathcal{H} := \tilde{H}^{-1/2}(\Gamma)$ and its dual $\mathcal{H}^* = H^{1/2}(\Gamma)$. It thus provides an equivalent scalar product $\langle\langle \cdot, \cdot \rangle\rangle$ on the energy space \mathcal{H} defined by $\langle\langle \phi, \psi \rangle\rangle := \langle V\phi, \psi \rangle$, where the duality brackets $\langle \cdot, \cdot \rangle$ extend the $L^2(\Gamma)$ -scalar product. We denote by $\|\cdot\|$ the induced energy norm.

Given $f \in \mathcal{H}^*$, the unique solution $\phi \in \mathcal{H}$ of (1.1) solves

$$(1.3) \quad \langle\langle \phi, \psi \rangle\rangle = \langle f, \psi \rangle \quad \text{for all } \psi \in \mathcal{H}.$$

Let $\mathcal{T}_h = \{T_1, \dots, T_N\}$ be a triangulation of Γ (with local mesh-size h). Then, the lowest-order Galerkin method is to find a \mathcal{T}_h -piecewise constant function $\phi_h \in X_h := \mathcal{P}^0(\mathcal{T}_h)$ which solves

$$(1.4) \quad \langle\langle \phi_h, \psi_h \rangle\rangle = \langle f, \psi_h \rangle \quad \text{for all } \psi_h \in X_h.$$

We stress the Galerkin orthogonality

$$(1.5) \quad \langle\langle \phi - \phi_h, \psi_h \rangle\rangle = 0 \quad \text{for all } \psi_h \in X_h,$$

which in fact characterizes the discrete solution $\phi_h \in X_h$.

The goal of this work is to contribute to the simple and accurate a posteriori estimation for the error $\|\phi - \phi_h\|$ in the energy norm: An a posteriori error estimator is a computable quantity η which does not depend on the (in general unknown) exact solution ϕ but on a computed discrete solution ϕ_h and which estimates the error $\|\phi - \phi_h\|$ in the energy norm. We aim to provide estimates

$$(1.6) \quad C_{\text{eff}}^{-1} \eta \leq \|\phi - \phi_h\| \leq C_{\text{rel}} \eta$$

which are referred to as efficiency (lower estimate) and reliability (upper estimate) of η , respectively. The constants $C_{\text{eff}}, C_{\text{rel}}$ may not depend on ϕ or ϕ_h , but on the given right-hand side $f \in \mathcal{H}^*$ as well as weakly on \mathcal{T}_h , e.g., on the local mesh-ratio $\kappa(\mathcal{T}_h)$. Moreover, two error estimators η and μ are said to be equivalent provided that

$$(1.7) \quad C_{\text{low}}^{-1} \mu \leq \eta \leq C_{\text{high}} \mu$$

with appropriate constants $C_{\text{low}}, C_{\text{high}} > 0$ which only depend on $\kappa(\mathcal{T}_h)$.

The content of the paper is organized as follows: The analysis of all error estimators introduced below, is based on so-called localization techniques which allow to replace the energy norm $\|\cdot\|$ by a weighted L^2 -norm $\|h^{1/2}(\cdot)\|_{L^2(\Gamma)}$. Notations, preliminaries, and the localization arguments are collected in Section 2. Section 3 is concerned with error estimation by space enrichment. In the simplest case, we are dealing with the h - $h/2$ -based error estimation [8]: Let $\phi_{h/2} \in X_{h/2} := \mathcal{P}^0(\mathcal{T}_{h/2})$ be an improved Galerkin solution, where the triangulation $\mathcal{T}_{h/2}$ is obtained from a uniform refinement of \mathcal{T}_h , i.e. $X_h \subset X_{h/2}$. Then,

$$(1.8) \quad \eta_{SH} = \|\phi_{h/2} - \phi_h\|$$

yields an efficient error estimator with efficiency constant $C_{\text{eff}} = 1$. Reliability of which holds under the saturation assumption (3.3) discussed below. The localization techniques of Section 2 provide an equivalent error estimator

$$(1.9) \quad \mu_{SH} = \|h^{1/2}(\phi_{h/2} - \phi_h)\|_{L^2(\Gamma)}$$

which can be employed for an indicator-based adaptive mesh-refinement. Section 4 treats the two-level error estimator introduced by Stephan and coworkers [15]: For an element $T_j \in \mathcal{T}_h$, let χ_j denote the corresponding characteristic function. Choosing another function $\varphi_j \in X_{h/2}$ which is orthogonal to χ_j in the L^2 -sense and which satisfies $\text{supp}(\varphi_j) = T_j$, we obtain an L^2 -orthogonal basis of $X_{h/2}$. With the one-dimensional space $X_{h,j} := \text{span}\{\varphi_j\}$ and $\mathbb{G}_{h,j}$ the Galerkin projection onto $X_{h,j}$, the two-level error estimator reads

$$(1.10) \quad \eta_{TH} = \left(\sum_{T_j \in \mathcal{T}_h} \eta_{TH,j}^2 \right)^{1/2}, \quad \text{where} \quad \eta_{TH,j} = \frac{|\langle f - V\phi_h, \varphi_j \rangle|}{\|\varphi_j\|}.$$

With the help of the localization techniques of Section 2, we show equivalency of η_{TH} and η_{SH} . Our proof generalizes the arguments of [15] from uniform to adaptively generated meshes. Finally, Section 5 recalls the averaging-based error estimator

$$(1.11) \quad \eta_A = \|\phi_{h/2} - \mathbb{G}_h^{(1)} \phi_{h/2}\|$$

from [3, 4], where $\mathbb{G}_h^{(1)}$ denotes the Galerkin projection onto the \mathcal{T}_h -piecewise affine but discontinuous functions $X_h^{(1)} := \mathcal{P}^1(\mathcal{T}_h)$. The localization techniques of Section 2 provide the

equivalent error estimator

$$(1.12) \quad \tilde{\mu}_A = \|h^{1/2}(\phi_{h/2} - \Pi_h^{(1)}\phi_{h/2})\|_{L^2(\Gamma)},$$

where $\Pi_h^{(1)}$ is the L^2 -projection onto $X_h^{(1)}$. Again, this implementationally simple error estimator can be used to steer an adaptive mesh-refining algorithm. Under rather strong assumptions discussed below, η_A (and thus $\tilde{\mu}_A$) is a reliable and efficient error estimator for the improved Galerkin error $\|\phi - \phi_{h/2}\|$. In this paper, we provide an elementary proof that η_A is always equivalent to η_{SH} . This may be seen as a first step to weaken the assumptions of [3, 4] and to mathematically explain the good performance of η_A in numerical computations. Numerical experiments in Section 6 conclude the work. As model examples serve the first-kind integral equations with weakly singular kernel which arise from the Dirichlet problems of the Laplace, the Lamé, and the Stokes problem, respectively.

2. PRELIMINARIES AND LOCALIZATION OF $\tilde{H}^{-1/2}$ -NORM

The analysis below only makes use of the following assumptions: We assume that $\langle\langle \cdot, \cdot \rangle\rangle$ is a given scalar product on $\tilde{H}^{-1/2}(\Gamma)$ which induces an equivalent norm $\|\cdot\|$ on $\tilde{H}^{-1/2}(\Gamma)$. This situation is met for several first-kind integral equations, which arise from elliptic PDEs. Other examples — besides the Laplace equation from the introduction — are given in the numerical experiments below. We then consider a variational formulation (1.3) for given data $f \in H^{1/2}(\Gamma)$. According to Riesz' theorem, there is a unique solution $\phi \in \tilde{H}^{-1/2}(\Gamma)$. With a conforming discrete space $X_h \subset \tilde{H}^{-1/2}(\Gamma)$, we consider the Galerkin method (1.4).

2.1. Galerkin Discretization. The focus of this work is on the lowest-order Galerkin scheme, where X_h denotes the space $\mathcal{P}^0(\mathcal{T}_h)$ of all \mathcal{T}_h -piecewise constant functions, where \mathcal{T}_h is a given triangulation \mathcal{T}_h of Γ . Here, triangulation means only that $\mathcal{T}_h = \{T_1, \dots, T_N\}$ is a finite set of connected and relatively open subsets of Γ such that $\bar{\Gamma} = \bigcup_{j=1}^N \bar{T}_j$. For the ease of presentation, we assume that the elements T_j are affine boundary pieces. We define the local mesh-width by

$$(2.1) \quad h \in L^\infty(\Gamma), \quad h|_{T_j} := h_j := \sup\{|x - y| : x, y \in T_j\}.$$

Moreover, the local mesh-ratio is given by

$$(2.2) \quad \kappa(\mathcal{T}_h) := \max\{h_j/h_k : T_j, T_k \in \mathcal{T}_h \text{ with } \bar{T}_j \cap \bar{T}_k \neq \emptyset\},$$

i.e. by the maximal quotient of the elements-widths of two neighbouring elements. Refinement of an element $T_j \in \mathcal{T}_h$ means that T_j is split into two new elements of half length. Since the error estimates below depend on $\kappa(\mathcal{T}_h)$, our implementation always ensures that $\kappa(\mathcal{T}_h) \leq 2$, i.e. an element T_j is automatically marked for refinement provided that it has a neighbour T_k with $h_j > 2h_k$.

2.2. Notational Conventions. If not stated otherwise, we use the following notation,

$$(2.3) \quad X_h := \mathcal{P}^0(\mathcal{T}_h), \quad X_{h/2} := \mathcal{P}^0(\mathcal{T}_{h/2}), \quad \text{and} \quad X_h^{(1)} := \mathcal{P}^1(\mathcal{T}_h),$$

where the triangulation $\mathcal{T}_{h/2}$ is obtained from a uniform refinement of \mathcal{T}_h . Moreover, in Section 3 and 4, we use

$$(2.4) \quad \hat{X}_h \in \{X_{h/2}, X_h^{(1)}\},$$

i.e. \widehat{X}_h denotes either $X_{h/2}$ or $X_h^{(1)}$. The Galerkin solutions with respect to X_h , $X_{h/2}$, $X_h^{(1)}$, and \widehat{X}_h are denoted by ϕ_h , $\phi_{h/2}$, $\phi_h^{(1)}$, and $\widehat{\phi}_h$, respectively. Throughout, Galerkin and L^2 -projections are denoted by

$$(2.5) \quad \mathbb{G} \quad \text{and} \quad \Pi,$$

respectively. The indices indicate the corresponding space, e.g. $\mathbb{G}_h^{(1)}$ denotes the Galerkin projection onto $X_h^{(1)}$ and $\Pi_{h/2}$ denotes the L^2 -projection onto $X_{h/2}$.

Altogether, we shall introduce fourteen different error estimators below. Throughout, the notation of the a posteriori error estimators

$$(2.6) \quad \eta, \quad \widetilde{\eta}, \quad \mu, \quad \text{and} \quad \widetilde{\mu}$$

therefore uses the following convention: η denotes an error estimator which is based on the energy norm, whereas μ denotes an error estimator which is based on an $h^{1/2}$ -weighted L^2 -norm. Moreover, η and μ need the computation of a certain Galerkin projection \mathbb{G} , whereas $\widetilde{\eta}$ and $\widetilde{\mu}$ are based on L^2 -projections Π , c.f. the definition of the averaging-based error estimators η_A in (5.2), $\widetilde{\eta}_A$ in (5.8), and μ_A as well as $\widetilde{\mu}_A$ in (5.9). The subscript indicates the type of error estimator, e.g. η_A shows that this error estimator is based on averaging.

2.3. Localization of $\widetilde{H}^{-1/2}$ -norm. The first lemma provides a localization of the energy norm for discrete functions $\psi_h \in L^2(\Gamma)$. Since $\|\cdot\|$ is an equivalent norm on $\widetilde{H}^{-1/2}(\Gamma)$, this localization is naturally given in terms of a mesh-size weighted L^2 -norm. The inverse estimate (2.7) is proven in [9]. The approximation estimates (2.8)–(2.9) are taken from [3].

Lemma 2.1. (i) *For any discrete function $\psi_h \in \mathcal{P}^p(\mathcal{T}_h)$ holds the inverse estimate*

$$(2.7) \quad \|h^{1/2}\psi_h\|_{L^2(\Gamma)} \leq C_1 \|\psi_h\|,$$

where the constant $C_1 > 0$ only depends on Γ , the polynomial degree $p \geq 0$, and the local mesh-ratio $\kappa(\mathcal{T}_h)$.

(ii) *Let X_h be a finite dimensional subspace of $L^2(\Gamma)$ which contains at least $\mathcal{P}^0(\mathcal{T}_h)$, and let Π_h denote the L^2 -projection onto X_h . Then,*

$$(2.8) \quad \|\psi - \Pi_h\psi\| \leq C_2 \min \{ \|h^{1/2}\psi\|_{L^2(\Gamma)}, \|h^{1/2}(\psi - \Pi_h\psi)\|_{L^2(\Gamma)} \} \quad \text{for all } \psi \in L^2(\Gamma),$$

where the constant $C_2 > 0$ only depends on Γ but not on the triangulation \mathcal{T}_h .

(iii) *Under the assumptions of (ii), let \mathbb{G}_h be the Galerkin projection onto X_h . Then,*

$$(2.9) \quad \|\psi - \mathbb{G}_h\psi\| \leq C_2 \min \{ \|h^{1/2}\psi\|_{L^2(\Gamma)}, \|h^{1/2}(\psi - \mathbb{G}_h\psi)\|_{L^2(\Gamma)} \} \quad \text{for all } \psi \in L^2(\Gamma)$$

with the constant C_2 from (ii).

Sketch of Proof. The local inverse estimate (2.7) is proven in [9, Proposition 2.9] in the form

$$\|h^\alpha\psi_h\|_{L^2(\Gamma)} \leq \widetilde{C}_1 \|\psi_h\|_{\widetilde{H}^{-\alpha}(\Gamma)} \quad \text{for all } \psi_h \in \mathcal{P}^p(\mathcal{T}_h),$$

where \widetilde{C}_1 depends only on $\alpha \geq 0$, $p \geq 0$, and $\kappa(\mathcal{T}_h)$. For $\alpha = 1/2$, norm equivalence on $\widetilde{H}^{-1/2}(\Gamma)$ proves (2.7). The local approximation estimate from [3, Theorem 4.1] reads

$$\|\psi - \Pi_h\psi\|_{\widetilde{H}^{-\alpha}(\Gamma)} \leq \widetilde{C}_2 \|h^\alpha\psi\|_{L^2(\Gamma)} \quad \text{for all } \psi \in L^2(\Gamma),$$

where the constant \widetilde{C}_2 depends only on $\alpha \geq 0$. For $\alpha = 1/2$, norm equivalence on $\widetilde{H}^{-1/2}(\Gamma)$ leads to

$$(2.10) \quad \|\psi - \Pi_h \psi\| \leq C_2 \|h^{1/2} \psi\|_{L^2(\Gamma)} \quad \text{for all } \psi \in L^2(\Gamma).$$

The strengthened form (2.8) is obtained by simple postprocessing: Note that the projection property $\Pi_h^2 = \Pi_h$ implies $\Psi := (1 - \Pi_h)\psi = (1 - \Pi_h)^2\psi = (1 - \Pi_h)\Psi$ for all $\psi \in L^2(\Gamma)$. Applying (2.10) to $\Psi \in L^2(\Gamma)$, we obtain

$$(2.11) \quad \|\psi - \Pi_h \psi\| = \|\Psi - \Pi_h \Psi\| \leq C_2 \|h^{1/2} \Psi\|_{L^2(\Gamma)} = C_2 \|h^{1/2}(\psi - \Pi_h \psi)\|_{L^2(\Gamma)}.$$

The combination of (2.10)–(2.11) proves (2.8). To prove (2.9), note that the best approximation property of the Galerkin projection yields, for $\psi \in L^2(\Gamma)$,

$$(2.12) \quad \|\psi - \mathbb{G}_h \psi\| \leq \|\psi - \Pi_h \psi\| \leq C_2 \|h^{1/2} \psi\|_{L^2(\Gamma)}.$$

By use of $\mathbb{G}_h^2 = \mathbb{G}_h$, we may apply the same arguments as for the L^2 -projection Π_h , to derive (2.9) from (2.12). \square

3. ERROR ESTIMATION BY SPACE ENRICHMENT

Let X_h and \widehat{X}_h be discrete subspaces of $\widetilde{H}^{-1/2}(\Gamma)$ with corresponding Galerkin solutions $\phi_h \in X_h$ and $\widehat{\phi}_h \in \widehat{X}_h$, respectively. We assume that $X_h \subset \widehat{X}_h$. Then, the best approximation property of the Galerkin solution with respect to the energy norm yields

$$(3.1) \quad \|\phi - \widehat{\phi}_h\| \leq \|\phi - \phi_h\|.$$

We now use the difference of the two Galerkin solutions

$$(3.2) \quad \eta_S := \|\widehat{\phi}_h - \phi_h\|$$

to estimate the error $\|\phi - \phi_h\|$. The Galerkin orthogonality (1.5) for \widehat{X}_h yields

$$\|\phi - \phi_h\|^2 = \|\phi - \widehat{\phi}_h\|^2 + \|\widehat{\phi}_h - \phi_h\|^2 = \|\phi - \widehat{\phi}_h\|^2 + \eta_S^2$$

and thus $\eta_S \leq \|\phi - \phi_h\|$. This proves efficiency of η_S with $C_{\text{eff}} = 1$. The reliability of η_S is usually proven with the help of the **saturation assumption**, which is a strengthened version of (3.1) and reads

$$(3.3) \quad \|\phi - \widehat{\phi}_h\| \leq q_S \|\phi - \phi_h\| \quad \text{with some uniform constant } q_S \in (0, 1).$$

Under this assumption, we obtain $\|\phi - \phi_h\|^2 = \|\phi - \widehat{\phi}_h\|^2 + \eta_S^2 \leq q_S^2 \|\phi - \phi_h\|^2 + \eta_S^2$ and thus reliability

$$(3.4) \quad \|\phi - \phi_h\| \leq \frac{1}{\sqrt{1 - q_S^2}} \eta_S.$$

We state these elementary observations in the following proposition.

Proposition 3.1. (i) *The error estimator η_S is always efficient with $C_{\text{eff}} = 1$.*
(ii) *Under the saturation assumption (3.3), η_S is reliable with $C_{\text{rel}} = 1/\sqrt{1 - q_S^2}$.* \square

Clearly, the space \widehat{X}_h has to be sufficiently larger than X_h to allow and guarantee (3.3). In the following, we consider two canonical choices for the enriched space \widehat{X}_h : First, the h - $h/2$ -strategy which has been studied in [8]. Let $\mathcal{T}_h = \{T_1, \dots, T_N\}$ be a triangulation of Γ

and $\mathcal{T}_{h/2}$ be obtained from a uniform refinement of \mathcal{T}_h . We then may consider the discrete spaces

$$(3.5) \quad X_h := \mathcal{P}^0(\mathcal{T}_h) \quad \text{and} \quad \widehat{X}_h := \mathcal{P}^0(\mathcal{T}_{h/2}).$$

Alternatively, we might use the analogous p -($p+1$)-strategy, where

$$(3.6) \quad X_h := \mathcal{P}^0(\mathcal{T}_h) \quad \text{and} \quad \widehat{X}_h := \mathcal{P}^1(\mathcal{T}_h).$$

For either of the two choices, the error estimator η_S suffers from two things: First, the energy norm $\|\cdot\|$ does not provide information, where the mesh \mathcal{T}_h should be refined to decrease the error most efficiently. Second, we do not only have to compute the Galerkin approximation ϕ_h with respect to X_h but even the computationally more expensive Galerkin solution $\widehat{\phi}_h$. A numerical algorithm clearly returns $\widehat{\phi}_h$. According to (3.1), this is a better approximation of the exact solution ϕ than ϕ_h .

A remedy for both is given by the following theorem which is proven in [8] for the h - $h/2$ -strategy (3.5). It essentially states the following: First, the nonlocal energy norm is replaced by an h -weighted L^2 -norm. Second, we might replace ϕ_h by the L^2 -projection $\Pi_h \widehat{\phi}_h$ of the more accurate Galerkin solution $\widehat{\phi}_h$. Instead of solving a linear system with dense Galerkin matrix to obtain ϕ_h , we thus only compute $\Pi_h \widehat{\phi}_h$, which is done in real linear complexity.

Theorem 3.2. *Let X_h and \widehat{X}_h be given by either (3.5) or (3.6). Besides the error estimator η_S , we define*

$$(3.7) \quad \widetilde{\eta}_S := \|\widehat{\phi}_h - \Pi_h \widehat{\phi}_h\|$$

as well as the h -weighted L^2 -norm based error estimators

$$(3.8) \quad \mu_S := \|h^{1/2}(\widehat{\phi}_h - \phi_h)\|_{L^2(\Gamma)} \quad \text{and} \quad \widetilde{\mu}_S := \|h^{1/2}(\widehat{\phi}_h - \Pi_h \widehat{\phi}_h)\|_{L^2(\Gamma)},$$

where Π_h denotes the L^2 -projection onto X_h . With the constants $C_1, C_2 > 0$ of Lemma 2.1, there hold the estimates

$$(3.9) \quad \widetilde{\mu}_S \leq \mu_S \leq \sqrt{2} C_1 \eta_S \quad \text{and} \quad \eta_S \leq \widetilde{\eta}_S \leq C_2 \widetilde{\mu}_S.$$

Therefore, all error estimators are always efficient, and reliability holds under the saturation assumption (3.3).

Proof. Let \mathbb{G}_h denote the Galerkin projection onto X_h . Note that $\mathbb{G}_h \widehat{\phi}_h = \phi_h$ according to $X_h \subset \widehat{X}_h$. Therefore the approximation property of the Galerkin projection and the approximation estimate (2.8) prove $\eta_S \leq \widetilde{\eta}_S \leq C_2 \widetilde{\mu}_S$. The estimate $\mu_S \leq \sqrt{2} C_1 \eta_S$ follows from the inverse estimate (2.7) applied for \widehat{X}_h , where the additional factor $\sqrt{2}$ arises in case of the h - $h/2$ -strategy. Finally, recall that according to the choice of X_h , the L^2 -orthogonal projection onto X_h is even the \mathcal{T}_h -elementwise orthogonal projection. This implies

$$h_{T_j} \|\widehat{\phi}_h - \Pi_h \widehat{\phi}_h\|_{L^2(T_j)}^2 \leq h_{T_j} \|\widehat{\phi}_h - \mathbb{G}_h \widehat{\phi}_h\|_{L^2(T_j)}^2 \quad \text{for all } T_j \in \mathcal{T}_h.$$

Summing these estimates over all elements $T_j \in \mathcal{T}_h$, we conclude $\widetilde{\mu}_S \leq \mu_S$. \square

Remark 1. (i) *The estimate $\eta_S \leq \widetilde{\eta}_S$ holds whenever $X_h \subseteq \widehat{X}_h \subset L^2(\Gamma)$.*

(ii) *The estimate $\mu_S \leq \sqrt{2} C_1 \eta_S$ holds for any spaces X_h and \widehat{X}_h as long as $\widehat{X}_h \subseteq \mathcal{P}^p(\mathcal{T}_h)$ for some polynomial degree $p \geq 0$ and some triangulation \mathcal{T}_h . The constant C_1 then depends on*

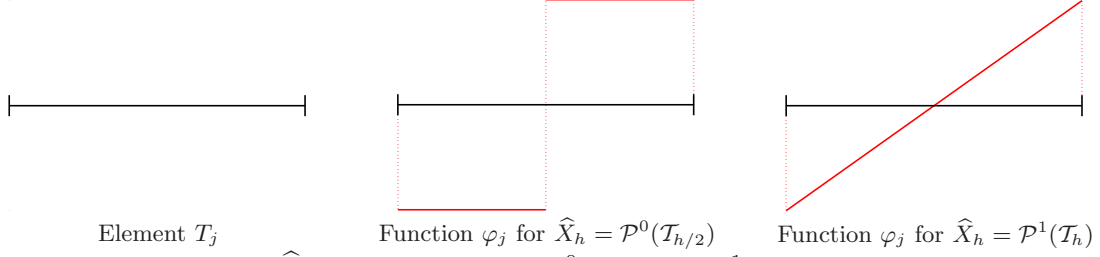


FIGURE 1. The space \widehat{X}_h , which is either $\mathcal{P}^0(\mathcal{T}_{h/2})$ or $\mathcal{P}^1(\mathcal{T}_h)$ is decomposed into the L^2 -orthogonal sum of $X_{h,0} = X_h = \mathcal{P}^0(\mathcal{T}_h)$ and the one-dimensional spaces $X_{h,j} := \text{span}\{\varphi_j\}$. In either case, the function φ_j is orthogonal to the characteristic function χ_{T_j} and has local support $\text{supp}(\varphi_j) \subseteq T_j$, and we assume that φ_j has minimum -1 and maximum $+1$.

the local mesh-ratio of \mathcal{T}_h .

(ii) The estimates $\eta_S \leq C_2 \mu_S$ and $\tilde{\eta}_S \leq C_2 \tilde{\mu}_S$ hold provided that $\mathcal{P}^0(\mathcal{T}_h) \subseteq X_h$.

(iii) Only the estimate $\tilde{\mu}_S \leq \mu_S$ depends on the special choice of X_h . \square

Remark 2. For the finite element method and the h - $h/2$ -strategy (3.5), the saturation assumption (3.3) can be proven under some mild conditions on the local mesh refinement [7]. However, we stress that the saturation assumption — although observed in praxis, cf. [8] — has not been proven for the boundary element method, yet. \square

The error estimator $\tilde{\mu}_S$ can be written in the form

$$(3.10) \quad \tilde{\mu}_S = \left(\sum_{j=1}^N \tilde{\mu}_{S,j}^2 \right)^{1/2},$$

where the local refinement indicators $\tilde{\mu}_{S,j} := h_{T_j}^{1/2} \|\widehat{\phi}_h - \Pi_h \widehat{\phi}_h\|_{L^2(T_j)}$ can be used for element marking in the following adaptive mesh-refining algorithm.

Algorithm 3.3. Input: Initial mesh \mathcal{T}_h , tolerance $\tau > 0$, adaptivity parameter $0 \leq \theta \leq 1$.

- (i) Compute Galerkin solution $\widehat{\phi}_h \in \widehat{X}_h$ and L^2 -projection $\Pi_h \widehat{\phi}_h \in X_h$.
- (ii) Stop provided that $\tilde{\eta}_S \leq \tau$.
- (iii) Otherwise, compute refinement indicators $\tilde{\mu}_{S,j}$ for all $T_j \in \mathcal{T}_h = \{T_1, \dots, T_N\}$.
- (iv) Mark elements $T_j \in \mathcal{T}_h$ with $\tilde{\mu}_{S,j} \geq \theta \max\{\tilde{\mu}_{S,k} : k = 1, \dots, N\}$ for refinement.
- (v) Refine all marked elements, generate a new mesh \mathcal{T}_h (satisfying the K -mesh property i.e. $\kappa(\mathcal{T}_h) \leq 2$), and goto (i)

Output: Galerkin approximation $\widehat{\phi}_h \in \widehat{X}_h$ and error estimator $\tilde{\eta}_S$, which is, however, supposed to control only the Galerkin error $\|\phi - \phi_h\|$ instead of $\|\phi - \widehat{\phi}_h\|$. \square

4. TWO-LEVEL ERROR ESTIMATION

Let $\mathcal{T}_h = \{T_1, \dots, T_N\}$ be a triangulation of Γ . Assume that the discrete spaces X_h and \widehat{X}_h are either given by (3.5) or by (3.6). Let $\phi_h \in X_h$ and $\widehat{\phi}_h \in \widehat{X}_h$ be the corresponding Galerkin solutions.

For each element $T_j \in \mathcal{T}_h$, we choose a function $\varphi_j \in \widehat{X}_h \setminus \{0\}$ with $\text{supp}(\varphi_j) \subseteq T_j$ and $\int_{T_j} \varphi_j ds = 0$, cf. Figure 1. Let $X_{h,0} := X_h$ and $X_{h,j} := \text{span}\{\varphi_j\}$ for $j = 1, \dots, N$. We denote with $\mathbb{G}_{h,j}$ and $\Pi_{h,j}$ the Galerkin projection and L^2 -projection onto $X_{h,j}$, respectively.

Lemma 4.1. *The spaces $X_{h,j}$ are pairwise L^2 -orthogonal for all $j = 0, \dots, N$. In particular, the L^2 -projection $\widehat{\Pi}_h$ onto \widehat{X}_h can be decomposed as $\widehat{\Pi}_h = \sum_{j=0}^N \Pi_{h,j}$.*

Proof. We consider $\mathcal{B} := \{\chi_{T_1}, \dots, \chi_{T_N}, \varphi_1, \dots, \varphi_N\}$. For $1 \leq j < k \leq N$, orthogonality of φ_j and φ_k follows from $\text{supp}(\varphi_\ell) \subseteq T_\ell$. Moreover, $\int_{T_\ell} \varphi_j ds = 0$ proves that φ_j is orthogonal to all characteristic functions χ_{T_ℓ} . Therefore, \mathcal{B} is an L^2 -orthogonal and hence linearly independent subset of \widehat{X}_h . Clearly, $\#\mathcal{B} = 2N = \dim \widehat{X}_h$ and $\text{span}(\mathcal{B}) \subseteq \widehat{X}_h$. Altogether, \mathcal{B} thus is an L^2 -orthogonal basis of \widehat{X}_h . The claims now follow from elementary Linear Algebra. \square

As a first consequence, we derive a representation of the error estimator $\widetilde{\mu}_S$ from the previous section.

Proposition 4.2. *With respect to the hierarchical basis, the error estimator $\widetilde{\mu}_S$ reads*

$$(4.1) \quad \widetilde{\mu}_S = \left(\sum_{j=1}^N h_{T_j} \|\Pi_{h,j} \widehat{\phi}_h\|_{L^2(T_j)}^2 \right)^{1/2}$$

Moreover, there holds

$$(4.2) \quad \|\Pi_{h,j} \widehat{\phi}_h\|_{L^2(T_j)} = \|\widehat{\phi}_h - \Pi_h \widehat{\phi}_h\|_{L^2(T_j)} = \frac{|\langle \widehat{\phi}_h, \varphi_j \rangle|}{\|\varphi_j\|_{L^2(T_j)}} \quad \text{for all } j = 1, \dots, N.$$

Proof. Using the orthogonal decomposition of $\widehat{\Pi}_h$ from Lemma 4.1, we obtain

$$\widehat{\phi}_h - \Pi_h \widehat{\phi}_h = \widehat{\Pi}_h(\widehat{\phi}_h - \Pi_h \widehat{\phi}_h) = \sum_{j=1}^N \Pi_{h,j}(\widehat{\phi}_h - \Pi_h \widehat{\phi}_h) = \sum_{j=1}^N \Pi_{h,j} \widehat{\phi}_h,$$

where the term for $j = 0$ vanishes since $\Pi_{h,0} = \Pi_h$. Together with $\text{supp}(\Pi_{h,j} \widehat{\phi}_h) \subseteq T_j$, this yields (4.1) as well as the first equality in (4.2). The second equality in (4.2) follows from the fact that an orthogonal projection can explicitly be written in terms of an orthogonal basis. In our case, the L^2 -projection $\Pi_{h,j}$ onto the one-dimensional space $X_{h,j} = \text{span}\{\varphi_j\}$ simply reads

$$\Pi_{h,j} \psi = \frac{\langle \psi, \varphi_j \rangle}{\|\varphi_j\|_{L^2(T_j)}^2} \varphi_j \quad \text{for all } \psi \in L^2(\Gamma).$$

This concludes the proof. \square

Lemma 4.3. *For any function $\widehat{\psi}_h \in \widehat{X}_h$ holds $\|\Pi_h \widehat{\psi}_h\| \leq C_3 \|\widehat{\psi}_h\|$, where the constant $C_3 > 0$ only depends on the constants $C_1, C_2 > 0$ of Lemma 2.1.*

Proof. Note that $\|(1 - \Pi_h) \widehat{\psi}_h\| \leq C_2 \|h^{1/2} \widehat{\psi}_h\|_{L^2(\Gamma)} \leq \sqrt{2} C_1 C_2 \|\widehat{\psi}_h\|$, where the pessimistic factor $\sqrt{2}$ arises in case of the h - $h/2$ -strategy (3.5). Therefore, the triangle inequality proves $\|\Pi_h \widehat{\psi}_h\| \leq (1 + \sqrt{2} C_1 C_2) \|\widehat{\psi}_h\|$. \square

Lemma 4.4. For any functions $\psi_j \in X_{h,j}$ holds

$$(4.3) \quad C_4^{-1} \left(\sum_{j=1}^N \|\psi_j\|^2 \right)^{1/2} \leq \left\| \sum_{j=1}^N \psi_j \right\| \leq C_5 \left(\sum_{j=1}^N \|\psi_j\|^2 \right)^{1/2},$$

where the constants $C_4, C_5 > 0$ only depend on the constants $C_1, C_2 > 0$ of Lemma 2.1.

Proof. Lemma 4.1 implies $\psi_j = (1 - \Pi_h)\psi_j$. With $\text{supp}(\psi_j) \subseteq T_j$, we thus infer

$$\|\psi_j\| = \|(1 - \Pi_h)\psi_j\| \leq C_2 \|h^{1/2}\psi_j\|_{L^2(\Gamma)} = C_2 \|h^{1/2}\psi_j\|_{L^2(T_j)}.$$

Summing these estimates over all $j = 1, \dots, N$, we obtain

$$\sum_{j=1}^N \|\psi_j\|^2 \leq C_2^2 \sum_{j=1}^N \|h^{1/2}\psi_j\|_{L^2(T_j)}^2 = C_2^2 \left\| h^{1/2} \sum_{j=1}^N \psi_j \right\|_{L^2(\Gamma)}^2 \leq 2 C_1^2 C_2^2 \left\| \sum_{j=1}^N \psi_j \right\|^2,$$

where we have used the local inverse estimate for $\widehat{\psi}_h = \sum_{j=1}^N \psi_j \in \widehat{X}_h$ in the final step. The converse inequality follows from the same type of arguments: With $\sum_{j=1}^N \psi_j = (1 - \Pi_h) \sum_{j=1}^N \psi_j$, we estimate

$$\left\| \sum_{j=1}^N \psi_j \right\|^2 \leq C_2^2 \left\| h^{1/2} \sum_{j=1}^N \psi_j \right\|_{L^2(\Gamma)}^2 = C_2^2 \sum_{j=1}^N \|h^{1/2}\psi_j\|_{L^2(T_j)}^2 \leq 2 C_1^2 C_2^2 \sum_{j=1}^N \|\psi_j\|^2,$$

where we have used that the supports $\text{supp}(\psi_j) \subseteq T_j$ are pairwise disjoint. \square

Proposition 4.5. For any function $\widehat{\psi}_h \in \widehat{X}_h$ holds

$$(4.4) \quad C_6^{-1} \|\widehat{\psi}_h\| \leq \left(\sum_{j=0}^N \|\mathbb{G}_{h,j}\widehat{\psi}_h\|^2 \right)^{1/2} \leq C_7 \|\widehat{\psi}_h\|$$

as well as

$$(4.5) \quad C_7^{-1} \|\widehat{\psi}_h\| \leq \left(\sum_{j=0}^N \|\Pi_{h,j}\widehat{\psi}_h\|^2 \right)^{1/2} \leq C_6 \|\widehat{\psi}_h\|,$$

where the constants $C_6, C_7 > 0$ only depend on the constants $C_3, C_5 > 0$ of Lemma 4.3 and Lemma 4.4.

Proof. According to Lemma 4.1 holds $\widehat{\psi}_h = \sum_{j=0}^N \Pi_{h,j}\widehat{\psi}_h$. Therefore, the Cauchy inequality yields

$$\begin{aligned} \|\widehat{\psi}_h\|^2 &= \sum_{j=0}^N \langle \widehat{\psi}_h, \Pi_{h,j}\widehat{\psi}_h \rangle = \sum_{j=0}^N \langle \mathbb{G}_{h,j}\widehat{\psi}_h, \Pi_{h,j}\widehat{\psi}_h \rangle \\ &\leq \left(\sum_{j=0}^N \|\mathbb{G}_{h,j}\widehat{\psi}_h\|^2 \right)^{1/2} \left(\sum_{j=0}^N \|\Pi_{h,j}\widehat{\psi}_h\|^2 \right)^{1/2} \end{aligned}$$

The latter estimate shows that the upper estimate in (4.4) provides the lower estimate in (4.5) and vice versa. It thus only remains to prove the two upper bounds. We start with the upper bound in (4.5): Note that the $L^2(\Gamma)$ -projection $\Pi_{h,j}$ onto $X_{h,j}$ is local in the sense that it

is even the $L^2(T_j)$ -projection. Therefore, $\|h^{1/2}\Pi_{h,j}\widehat{\psi}_h\|_{L^2(T_j)} \leq \|h^{1/2}\widehat{\psi}_h\|_{L^2(T_j)}$. The same arguments as in the proof of Lemma 4.4 now lead to $\sum_{j=1}^N \|\Pi_{h,j}\widehat{\psi}_h\|^2 \leq C_5^2 \|\widehat{\psi}_h\|^2$. Together with Lemma 4.3, we thus obtain the upper bound

$$\sum_{j=0}^N \|\Pi_{h,j}\widehat{\psi}_h\|^2 \leq \max\{C_3, C_5\}^2 \|\widehat{\psi}_h\|^2$$

and consequently the lower bound $\|\widehat{\psi}_h\|^2 \leq \max\{C_3, C_5\}^2 \sum_{j=0}^N \|\mathbb{G}_{h,j}\widehat{\psi}_h\|^2$. It remains to prove the upper bound in (4.4): A triangle inequality $\|\sum_{j=0}^N \mathbb{G}_{h,j}\widehat{\psi}_h\| \leq \|\mathbb{G}_{h,0}\widehat{\psi}_h\| + \|\sum_{j=1}^N \mathbb{G}_{h,j}\widehat{\psi}_h\| \leq \sqrt{2} (\|\mathbb{G}_{h,0}\widehat{\psi}_h\|^2 + \|\sum_{j=1}^N \mathbb{G}_{h,j}\widehat{\psi}_h\|^2)^{1/2}$ and Lemma 4.4 prove

$$\left\| \sum_{j=0}^N \mathbb{G}_{h,j}\widehat{\psi}_h \right\| \leq \sqrt{2} \max\{1, C_5\} \left(\sum_{j=0}^N \|\mathbb{G}_{h,j}\widehat{\psi}_h\|^2 \right)^{1/2}.$$

Therefore, the symmetry of the Galerkin projection yields

$$\sum_{j=0}^N \|\mathbb{G}_{h,j}\widehat{\psi}_h\|^2 = \sum_{j=0}^N \langle \mathbb{G}_{h,j}\widehat{\psi}_h, \widehat{\psi}_h \rangle \leq \left\| \sum_{j=0}^N \mathbb{G}_{h,j}\widehat{\psi}_h \right\| \|\widehat{\psi}_h\|.$$

The combination of the last two estimates proves the upper bound

$$\sum_{j=0}^N \|\mathbb{G}_{h,j}\widehat{\psi}_h\|^2 \leq \sqrt{2} \max\{1, C_5\}^2 \|\widehat{\psi}_h\|^2$$

and consequently even the lower bound $\|\widehat{\psi}_h\|^2 \leq \sqrt{2} \max\{1, C_5\}^2 \sum_{j=0}^N \|\Pi_{h,j}\widehat{\psi}_h\|^2$. \square

The following theorem has been proven by MUND-STEPHAN-WEISSE [15] for uniform mesh-refinement in 2D and 3D. We now generalize their proof to the case of adaptive mesh-refinement in 2D.

Theorem 4.6. *With the constants $C_6, C_7 > 0$ of Proposition 4.5, there holds*

$$(4.6) \quad C_6^{-1} \eta_S \leq \left(\sum_{j=1}^N \|\mathbb{G}_{h,j}(\widehat{\phi}_h - \phi_h)\|^2 \right)^{1/2} \leq C_7 \eta_S,$$

where η_S denotes the error estimator from the previous section. In particular, with the refinement indicators $\eta_{T,j} := \|\mathbb{G}_{h,j}(\widehat{\phi}_h - \phi_h)\|$, the two-level error estimator $\eta_T := \left(\sum_{j=1}^N \eta_{T,j}^2 \right)^{1/2}$ is equivalent to η_S . Therefore, η_T is always efficient, and reliability of η_T holds under the saturation assumption (3.3). Finally, $\eta_{T,j}$ can be written as

$$(4.7) \quad \eta_{T,j} = \frac{|\langle \widehat{\phi}_h - \phi_h, \varphi_j \rangle|}{\|\varphi_j\|} = \frac{|\langle f - V\phi_h, \varphi_j \rangle|}{\|\varphi_j\|} \quad \text{for } j = 1, \dots, N.$$

Proof. We simply apply Proposition 4.5 for $\widehat{\psi}_h = \widehat{\phi}_h - \phi_h \in \widehat{X}_h$, where the term for $j = 0$ vanishes due to $\mathbb{G}_h\widehat{\phi}_h = \phi_h$. This proves (4.6), and it remains to verify (4.7): The second equality $\langle \widehat{\phi}_h - \phi_h, \varphi_j \rangle = \langle f - V\phi_h, \varphi_j \rangle$ follows from the Galerkin equations (1.3) for \widehat{X}_h

and the definition of the energy scalar product. The first equality in (4.7) follows from the explicit representation of the orthogonal projection $\mathbb{G}_{h,j}$ which reads

$$\mathbb{G}_{h,j}\psi = \frac{\langle\langle \psi, \varphi_j \rangle\rangle}{\|\|\varphi_j\|\|^2} \varphi_j \quad \text{for all } \psi \in H^{-1/2}(\Gamma).$$

This concludes the proof. \square

The adaptive mesh-refining algorithm 3.3, is slightly modified and takes now the following form:

Algorithm 4.7. Input: *Initial mesh* \mathcal{T}_h , *tolerance* $\tau > 0$, *adaptivity parameter* $0 \leq \theta \leq 1$.

- (i) *Compute Galerkin solution* $\phi_h \in X_h$.
- (ii) *Compute refinement indicators* $\eta_{T,j}$ for all $T_j \in \mathcal{T}_h = \{T_1, \dots, T_N\}$.
- (iii) *Stop provided that* $\eta_T := \left(\sum_{j=1}^N \eta_{T,j}^2\right)^{1/2} \leq \tau$.
- (iv) *Otherwise, mark all* $T_j \in \mathcal{T}_h$ *with* $\eta_{T,j} \geq \theta \max\{\eta_{T,k} : k = 1, \dots, N\}$ *for refinement.*
- (v) *Refine all marked elements, generate a new mesh* \mathcal{T}_h *(satisfying the K-mesh property i.e. $\kappa(\mathcal{T}_h) \leq 2$), and goto (i)*

Output: *Galerkin approximation* $\phi_h \in X_h$ *and error estimator* η_T . \square

Remark 3. *Compared with the error estimators of the previous section, the two-level error estimator η_T has two mayor advantages: First, there is no overshooting in the sense that we compute and control the Galerkin approximation $\phi_h \in X_h$. We do not have to compute the improved Galerkin approximation $\hat{\phi}_h \in \hat{X}_h$. Nevertheless, the computation of the refinement indicators $\eta_{T,j}$ enforces to build the Galerkin matrix with respect to \hat{X}_h . Second, in case of $\hat{X}_h = \mathcal{P}^0(\mathcal{T}_{h/2})$, the refinement indicators $\eta_{T,j}$ are natural in the sense that they control the local Galerkin error and measure the improvement if we enrich X_h by the two-level basis function $\varphi_j \in \hat{X}_h$. \square*

5. AVERAGING ON LARGE PATCHES

One drawback of the error estimators of Section 3 and 4 is that we have to compute the improved Galerkin solution $\hat{\phi}_h \in \hat{X}_h$, whereas the error estimates only control with the error $\|\|\phi - \phi_h\|\|$ for the Galerkin solution $\phi_h \in X_h = \mathcal{P}^0(\mathcal{T}_h)$. This will be different for the error estimator discussed in this section, where $\hat{X}_h = \mathcal{P}^0(\mathcal{T}_{h/2})$ and where we aim to control $\|\|\phi - \hat{\phi}_h\|\|$: Let $\mathcal{T}_h = \{T_1, \dots, T_N\}$ be a given triangulation of Γ and $\mathcal{T}_{h/2}$ obtained by a uniform refinement of \mathcal{T}_h . We use the spaces

$$(5.1) \quad X_{h/2} := \mathcal{P}^0(\mathcal{T}_{h/2}) \quad \text{and} \quad X_h^{(1)} := \mathcal{P}^1(\mathcal{T}_h)$$

with corresponding Galerkin solutions $\phi_{h/2} \in X_{h/2}$ and $\phi_h^{(1)} \in X_h^{(1)}$, respectively. In a first step, we consider the error estimator

$$(5.2) \quad \eta_A := \|\|\phi_{h/2} - \mathbb{G}_h^{(1)}\phi_{h/2}\|\|,$$

where $\mathbb{G}_h^{(1)}$ denotes the Galerkin projection onto $X_h^{(1)}$. We stress, however, that this error estimator is computationally challenging because of the expensive Galerkin projection $\mathbb{G}_h^{(1)}$. The following theorem is proven in [3, 4].

Theorem 5.1. *The error estimator η_A satisfies*

$$(5.3) \quad \eta_A - \|\phi - \phi_h^{(1)}\| \leq \|\phi - \phi_{h/2}\|.$$

Moreover, under the assumption

$$(5.4) \quad \lambda_A := \max_{\psi_h^{(1)} \in X_h^{(1)}} \min_{\psi_{h/2} \in X_{h/2}} \frac{\|\psi_h^{(1)} - \psi_{h/2}\|}{\|\psi_h^{(1)}\|} < 1$$

holds the a posteriori error estimate

$$(5.5) \quad \|\phi - \phi_{h/2}\| \leq \frac{1}{\sqrt{1 - \lambda_A^2}} (\eta_A + \|\phi - \phi_h^{(1)}\|).$$

Therefore, η_A is reliable and efficient with respect to $\|\phi - \phi_{h/2}\|$ up to the higher-order Galerkin error $\|\phi - \phi_h^{(1)}\|$. \square

The following corollary is an immediate consequence:

Corollary 5.2. *With $q_A := \|\phi - \phi_h^{(1)}\| / \|\phi - \phi_{h/2}\|$, there holds efficiency*

$$(5.6) \quad \eta_A \leq (1 + q_A) \|\phi - \phi_{h/2}\|.$$

Provided that $\lambda_A^2 + q_A^2 < 1$, there even holds reliability

$$(5.7) \quad \|\phi - \phi_{h/2}\| \leq \frac{1}{\sqrt{1 - \lambda_A^2 - q_A}} \eta_A,$$

where λ_A denotes the constant from (5.4).

Proof. It only remains to prove (5.7): Note that $\lambda_A^2 + q_A^2 < 1$ implies $q_A / \sqrt{1 - \lambda_A^2} < 1$ as well as $\sqrt{1 - \lambda_A^2} - q_A > 0$. By definition of q_A , (5.5) implies

$$\left(1 - \frac{q_A}{\sqrt{1 - \lambda_A^2}}\right) \|\phi - \phi_{h/2}\| \leq \frac{1}{\sqrt{1 - \lambda_A^2}} \eta_A,$$

where the constant on the left-hand side may be written as $(\sqrt{1 - \lambda_A^2} - q_A) / \sqrt{1 - \lambda_A^2}$. \square

Remark 4. *We stress that neither Assumption (5.4) nor the stronger version $\lambda_A^2 + q_A^2 < 1$ can seriously be checked in praxis. Due to Lemma 2.1, however, there holds*

$$\min_{\psi_H \in X_H} \|\psi_h^{(1)} - \psi_H\| \leq C_2 \|H^{1/2} \psi_h^{(1)}\|_{L^2(\Gamma)} \leq C_1 C_2 \|H/h\|_{L^\infty(\Gamma)}^{1/2} \|\psi_h^{(1)}\| \quad \text{for all } \psi_h^{(1)} \in X_h^{(1)}$$

as long as $\mathcal{P}^0(\mathcal{T}_H) \subseteq X_H$. If \mathcal{T}_H is obtained from $\ell \in \mathbb{N}$ uniform refinements of \mathcal{T}_h , there holds $\|H/h\|_{L^\infty(\Gamma)} = 2^{-\ell}$. In this case, we observe

$$\max_{\psi_h^{(1)} \in X_h^{(1)}} \min_{\psi_H \in X_H} \frac{\|\psi_h^{(1)} - \psi_H\|}{\|\psi_h^{(1)}\|} \leq 2^{-\ell/2} C_1 C_2 < 1$$

for ℓ sufficiently large. The numerical experiments in [3, 4] give experimental evidence that $\ell = 1$, i.e. $H = h/2$, might be sufficient. \square

Remark 5. (i) *For a \mathcal{T}_h -piecewise smooth exact solution $\phi \in H^{1+\varepsilon}(\mathcal{T}_h)$ and uniform mesh-refinement, the Galerkin error $\|\phi - \phi_h^{(1)}\|$ is of order $\mathcal{O}(h^{3/2+\varepsilon})$ and hence of higher order*

when compared to $\|\phi - \phi_{h/2}\| = \mathcal{O}(h^{3/2})$.

(ii) The numerical experiments of [3, 4], show that, even for a nonsmooth exact solution ϕ , there holds $q_A < 1$, i.e. it pays to use higher-order elements on a coarser mesh if compared to lower-order elements on a finer mesh. Moreover, for adaptive mesh-refinement, one observes convergence $q_A \rightarrow 0$.

(iii) In all numerical experiments from [3, 4], we observe efficiency and reliability of η_A . \square

The same arguments as in the proof of Theorem 3.2 apply to the localization of the averaging error estimator η_A . The following theorem is already stated in [4, Theorem 6.2].

Theorem 5.3. Besides the averaging error estimator η_A , we define

$$(5.8) \quad \tilde{\eta}_A := \|\phi_{h/2} - \Pi_h^{(1)} \phi_{h/2}\|$$

as well as the h -weighted L^2 -norm based error estimators

$$(5.9) \quad \mu_A := \|h^{1/2}(\phi_{h/2} - \mathbb{G}_h^{(1)} \phi_{h/2})\|_{L^2(\Gamma)} \quad \text{and} \quad \tilde{\mu}_A := \|h^{1/2}(\phi_{h/2} - \Pi_h^{(1)} \phi_{h/2})\|_{L^2(\Gamma)},$$

where $\Pi_h^{(1)}$ denotes the L^2 -projection onto $X_h^{(1)}$. With the constants $C_1, C_2 > 0$ of Lemma 2.1, there hold the estimates

$$(5.10) \quad \tilde{\mu}_A \leq \mu_A \leq \sqrt{2} C_1 \eta_A \quad \text{and} \quad \eta_A \leq \tilde{\eta}_A \leq C_2 \tilde{\mu}_A.$$

and thus equivalency of the error estimators $\eta_A, \tilde{\eta}_A, \mu_A$, and $\tilde{\mu}_A$. \square

As in Section 3, the error estimator $\tilde{\mu}_A$ can be written in the form

$$(5.11) \quad \tilde{\mu}_A = \left(\sum_{j=1}^N \tilde{\mu}_{A,j}^2 \right)^{1/2},$$

where the local refinement indicators $\tilde{\mu}_{A,j} := h_{T_j}^{1/2} \|\phi_{h/2} - \Pi_h^{(1)} \phi_{h/2}\|_{L^2(T_j)}$ can be used for element marking in an adaptive mesh-refining strategy. The following adaptive algorithm is proposed in [3] and performs well in practice.

Algorithm 5.4. Input: Initial mesh \mathcal{T}_h , tolerance $\tau > 0$, adaptivity parameter $0 \leq \theta \leq 1$.

- (i) Refine mesh \mathcal{T}_h uniformly to obtain $\mathcal{T}_{h/2}$.
- (ii) Compute Galerkin solution $\phi_{h/2} \in X_{h/2}$ and L^2 -projection $\Pi_h^{(1)} \phi_{h/2} \in X_h^{(1)}$.
- (iii) Stop provided that $\tilde{\eta}_A \leq \tau$.
- (iv) Otherwise, compute refinement indicators $\tilde{\mu}_{A,j}$ for all $T_j \in \mathcal{T}_h = \{T_1, \dots, T_N\}$.
- (v) Mark elements $T_j \in \mathcal{T}_h$ with $\tilde{\mu}_{A,j} \geq \theta \max\{\tilde{\mu}_{A,k} : k = 1, \dots, N\}$ for refinement.
- (vi) Refine all marked elements, generate a new mesh \mathcal{T}_h (satisfying the K -mesh property i.e. $\kappa(\mathcal{T}_h) \leq 2$), and goto (i)

Output: Galerkin approximation $\phi_{h/2} \in X_{h/2}$ and error estimator $\tilde{\eta}_A$, which is empirically observed to control the Galerkin error $\|\phi - \phi_{h/2}\|$. \square

So far, we have seen that η_A as well as its modifications $\tilde{\eta}_A, \mu_A$, and $\tilde{\mu}_A$ might be expected to be reliable and efficient error estimators with respect to the energy error $\|\phi - \phi_{h/2}\|$. However, the mathematical justification of this is based on the strong assumption $\lambda_A^2 + q_A^2 < 1$. Since the error estimator η_A performs well in practice, we try to understand η_A with respect to

the error estimation of $\|\phi - \phi_h\|$. The following theorem states that η_A is equivalent to the h - $h/2$ -based error estimators from Section 3.

Theorem 5.5. *Let $\phi_h \in X_h := \mathcal{P}^0(\mathcal{T}_h)$ be the Galerkin solution with respect to X_h , and let Π_h denote the L^2 -projection onto X_h . Then, there holds*

$$(5.12) \quad \eta_A \leq \eta_{SH} := \|\phi_{h/2} - \phi_h\| \quad \text{as well as} \quad 2\tilde{\mu}_A = \tilde{\mu}_{SH} := \|h^{1/2}(\phi_{h/2} - \Pi_h\phi_{h/2})\|_{L^2(\Gamma)}$$

with the h - $h/2$ -based error estimators η_{SH} and $\tilde{\mu}_{SH}$ from Section 3. In particular, the averaging error estimators from Theorem 5.3 and the h - $h/2$ -error estimators from Theorem 3.2 are equivalent. In particular, the averaging error estimators are always efficient with respect to $\|\phi - \phi_h\|$, and reliability holds under the saturation assumption for the spaces X_h and $X_{h/2}$.

Proof. Let \mathbb{G}_h denote the Galerkin projection onto X_h . With the inclusion $X_h \subseteq X_h^{(1)}$, the Pythagoras theorem implies, for $\psi \in \tilde{H}^{-1/2}(\Gamma)$,

$$\|\psi - \mathbb{G}_h^{(1)}\psi\|^2 + \|\mathbb{G}_h^{(1)}\psi - \mathbb{G}_h\psi\|^2 = \|\psi - \mathbb{G}_h\psi\|^2.$$

For $\psi = \phi_{h/2}$, this equality reads $\eta_A^2 + \|\mathbb{G}_h^{(1)}\phi_{h/2} - \phi_h\|^2 = \eta_{SH}^2$, and we obtain the first estimate in (5.12). To prove $2\tilde{\mu}_A = \tilde{\mu}_{SH}$, it remains to prove that, for all elements $T_j \in \mathcal{T}_h$,

$$4\|\phi_{h/2} - \Pi_h^{(1)}\phi_{h/2}\|_{L^2(T_j)}^2 = \|\phi_{h/2} - \Pi_h\phi_{h/2}\|_{L^2(T_j)}^2$$

Since Π_h and $\Pi_h^{(1)}$ are even the elementwise L^2 -projections, the Pythagoras theorem proves

$$(5.13) \quad \|\psi - \Pi_h^{(1)}\psi\|_{L^2(T_j)}^2 + \|\Pi_h^{(1)}\psi - \Pi_h\psi\|_{L^2(T_j)}^2 = \|\psi - \Pi_h\psi\|_{L^2(T_j)}^2,$$

for all $\psi \in L^2(\Gamma)$. To compute the L^2 -norms, let $\varphi_j \in X_{h/2}$ and $\varphi_j^{(1)} \in X_h^{(1)}$ be the two-level basis functions from Figure 1. Note that L^2 -orthogonality of χ_{T_j} and $\varphi_j^{(1)}$ yields

$$\|\Pi_h^{(1)}\psi - \Pi_h\psi\|_{L^2(T_j)}^2 = \frac{\langle \psi, \varphi_j^{(1)} \rangle^2}{\|\varphi_j^{(1)}\|_{L^2(T_j)}^2}.$$

Moreover, L^2 -orthogonality of χ_{T_j} and φ_j proves, for $\psi \in \mathcal{P}^0(\mathcal{T}_{h/2})$,

$$\|\psi - \Pi_h\psi\|_{L^2(T_j)}^2 = \frac{\langle \psi, \varphi_j \rangle^2}{\|\varphi_j\|_{L^2(T_j)}^2}.$$

With the arc-length parametrization of T_j , we may assume that T_j is just the real interval $[0, h_j]$. If $\psi = \phi_{h/2}$ takes the values x on the interval $[0, h_j/2]$ and y on the interval $[h_j/2, h_j]$, elementary calculations prove

$$\langle \psi, \varphi_j \rangle = \frac{h_j}{2}(y - x), \quad \|\varphi_j\|_{L^2(T_j)}^2 = h_j \quad \text{and} \quad \langle \psi, \varphi_j^{(1)} \rangle = \frac{h_j}{4}(y - x), \quad \|\varphi_j^{(1)}\|_{L^2(T_j)}^2 = \frac{h_j}{3}.$$

We therefore obtain

$$\frac{3}{4}\|\psi - \Pi_h\psi\|_{L^2(T_j)}^2 = \frac{3h_j}{16}(y - x)^2 = \|\Pi_h^{(1)}\psi - \Pi_h\psi\|_{L^2(T_j)}^2.$$

Consequently, (5.13) implies

$$\|\psi - \Pi_h^{(1)}\psi\|_{L^2(T_j)}^2 = \frac{1}{4}\|\psi - \Pi_h\psi\|_{L^2(T_j)}^2,$$

from which we finally conclude $\tilde{\mu}_A = \tilde{\mu}_{SH}/2$. □

6. NUMERICAL EXPERIMENTS

We consider three numerical examples, namely the Galerkin boundary element method for the weakly singular integral equation for the Laplace, the Lamé, and the Stokes problem. In all examples, we choose the interval $\Gamma = (0, 1)$, the right hand side $f = 1$ resp. $f = (1, 1)^\top$, and lowest-order boundary elements, namely $\mathcal{P}^0(\mathcal{T}_h)$ resp. $\mathcal{P}^0(\mathcal{T}_h)^2$. We compare uniform mesh-refinement with an indicator-based adaptive mesh-refinement. For adaptive mesh-refinement, we use the local contributions of the introduced μ -estimators as well as of the two-level error estimators η_{TH} and η_{TP} . The respective adaptive strategies are stated above in Algorithm 3.3, Algorithm 4.7, and Algorithm 5.4, respectively. The subsequent section provides a short overview on the error estimators introduced in Section 3–5.

6.1. Overview on Introduced Error Estimators. Let $\mathcal{T}_h = \{T_1, \dots, T_N\}$ be a given triangulation of Γ and $\mathcal{T}_{h/2}$ be a uniform refinement of \mathcal{T}_h . Together with the spaces

$$X_h = \mathcal{P}^0(\mathcal{T}_h), \quad X_{h/2} = \mathcal{P}^0(\mathcal{T}_{h/2}), \quad \text{and} \quad X_h^{(1)} = \mathcal{P}^1(\mathcal{T}_h)$$

and corresponding Galerkin solutions ϕ_h , $\phi_{h/2}$, and $\phi_h^{(1)}$, respectively, we consider the following fourteen error estimators introduced above:

- the h - $h/2$ -based error estimators

$$\begin{aligned} \eta_{SH} &= \|\phi_{h/2} - \phi_h\|, & \mu_{SH} &= \|h^{1/2}(\phi_{h/2} - \phi_h)\|_{L^2(\Gamma)}, \\ \tilde{\eta}_{SH} &= \|\phi_{h/2} - \Pi_h \phi_{h/2}\|, & \tilde{\mu}_{SH} &= \|h^{1/2}(\phi_{h/2} - \Pi_h \phi_{h/2})\|_{L^2(\Gamma)}, \end{aligned}$$

- the h - $h/2$ -based two-level error estimator

$$\eta_{TH} = \left(\sum_{T \in \mathcal{T}_h} \eta_{TH,j}^2 \right)^{1/2} \quad \text{with} \quad \eta_{TH,j} = |\langle f - V\phi_h, \varphi_j \rangle| / \|\varphi_j\|,$$

- the averaging-based error estimators

$$\begin{aligned} \eta_A &= \|\phi_{h/2} - \mathbb{G}_h^{(1)} \phi_{h/2}\|, & \mu_A &= \|h^{1/2}(\phi_{h/2} - \mathbb{G}_h^{(1)} \phi_{h/2})\|_{L^2(\Gamma)}, \\ \tilde{\eta}_A &= \|\phi_{h/2} - \Pi_h^{(1)} \phi_{h/2}\|, & \tilde{\mu}_A &= \|h^{1/2}(\phi_{h/2} - \Pi_h^{(1)} \phi_{h/2})\|_{L^2(\Gamma)}, \end{aligned}$$

- the p - $(p+1)$ -based error estimators

$$\begin{aligned} \eta_{SP} &= \|\phi_h^{(1)} - \phi_h\|, & \mu_{SP} &= \|h^{1/2}(\phi_h^{(1)} - \phi_h)\|_{L^2(\Gamma)}, \\ \tilde{\eta}_{SP} &= \|\phi_h^{(1)} - \Pi_h \phi_h^{(1)}\|, & \tilde{\mu}_{SP} &= \|h^{1/2}(\phi_h^{(1)} - \Pi_h \phi_h^{(1)})\|_{L^2(\Gamma)}, \end{aligned}$$

- the p - $(p+1)$ -based two-level error estimator

$$\eta_{TP} = \left(\sum_{T \in \mathcal{T}_h} \eta_{TP,j}^2 \right)^{1/2} \quad \text{with} \quad \eta_{TP,j} = |\langle f - V\phi_h, \varphi_j^{(1)} \rangle| / \|\varphi_j^{(1)}\|.$$

Here, Π_h denotes the L^2 -projection onto X_h , and $\Pi_h^{(1)}$ and $\mathbb{G}_h^{(1)}$ denote the L^2 -projection and Galerkin projection onto $X_h^{(1)}$, respectively. The two-level basis functions $\varphi_j \in X_{h/2}$ and $\varphi_j^{(1)} \in X_h^{(1)}$ are shown in Figure 1 above. Note that the six global error estimators η_{SH} , $\tilde{\eta}_{SH}$, η_A , $\tilde{\eta}_A$, η_{SP} , and $\tilde{\eta}_{SP}$ can only be employed for error estimation, whereas the local

contributions of the remaining eight error estimators are used for the marking step of the adaptive mesh-refining algorithms.

We recall the equivalency of the five h - $h/2$ -based and the four averaging based error estimators. In particular, we have the following estimates with known constant 1,

$$\eta_A \leq \eta_{SH} \leq \tilde{\eta}_{SH}, \quad \eta_A \leq \tilde{\eta}_A, \quad \tilde{\mu}_A/2 = \tilde{\mu}_{SH} \leq \mu_{SH}, \quad \tilde{\mu}_A \leq \mu_A,$$

where the μ -estimates even hold \mathcal{T}_h -elementwise. The remaining equivalency estimates depend on the inverse estimate (2.7) or the approximation estimates (2.8)–(2.9), and so does the equivalency with η_{TH} . According to theory, these estimators are always efficient, whereas reliability holds provided that the saturation constant satisfies $q_{SH} := \|\phi - \phi_{h/2}\| / \|\phi - \phi_h\| < 1$. In particular, we then have the following estimate

$$\eta_A \leq \eta_{SH} \leq \|\phi - \phi_h\| \leq \frac{1}{\sqrt{1 - q_{SH}^2}} \eta_{SH}.$$

The analogous results for the p - $(p+1)$ -based error estimators read as follows: All five error estimators are equivalent and always efficient. We stress the estimates with known constant 1, namely

$$\eta_{SP} \leq \tilde{\eta}_{SP} \quad \text{and} \quad \tilde{\mu}_{SP} \leq \mu_{SP},$$

whereas the remaining equivalency estimates again depend on (2.7)–(2.9). The error estimators are always efficient and moreover reliable provided that the saturation constant satisfies $q_{SP} := \|\phi - \phi_h^{(1)}\| / \|\phi - \phi_h\| < 1$, namely

$$\eta_{SP} \leq \|\phi - \phi_h\| \leq \frac{1}{\sqrt{1 - q_{SP}^2}} \eta_{SP}.$$

Note that proper mesh-gradient should lead to convergence $q_{SP} \rightarrow 0$, since then $\|\phi - \phi_h\| = \mathcal{O}(N^{-3/2})$ and $\|\phi - \phi_h^{(1)}\| = \mathcal{O}(N^{-5/2})$ with respect to the number N of elements. Therefore, we expect η_{SP} to be asymptotically exact in case of adaptive mesh-refinement.

Finally, we stress that η_A additionally satisfies

$$\frac{1}{1 + q_A} \eta_A \leq \|\phi - \phi_{h/2}\| \leq \frac{1}{\sqrt{1 - \lambda_A^2 - q_A}} \eta_A$$

provided that $\lambda_A^2 + q_A^2 < 1$, where $q_A := q_{SP}/q_{SH}$ and where λ_A^2 is defined in (5.4). Under this assumption, η_A thus is a reliable and efficient estimator for the improved Galerkin error $\|\phi - \phi_{h/2}\|$.

6.2. Numerical Aspects. The entries of the Galerkin matrices are essentially of the type $I_{jk} = \int_{T_j} \int_{T_k} \log|x - y| ds_x ds_y$, for two elements $T_j, T_k \in \mathcal{T}_h$. We stress that these entries can be computed analytically [1, 14]. However, we found that is an issue of stability to use numerical quadrature for certain farfield entries. To be more precise, let $m_j, m_k \in \mathbb{R}^2$ be the midpoints of the elements T_j and T_k and $h_j, h_k > 0$ the corresponding element-widths. Provided $|m_j - m_k| > 16 \min\{h_j, h_k\}$, we computed I_{jk} by a 16×16 point tensorial Gauss quadrature. Otherwise, we used the analytic formulae of [14].

Throughout, the Galerkin errors $\|\phi - \phi_h\|$ are computed by use of the Galerkin orthogonality

$$\|\phi - \phi_h\|^2 = \|\phi\|^2 - \|\phi_h\|^2.$$

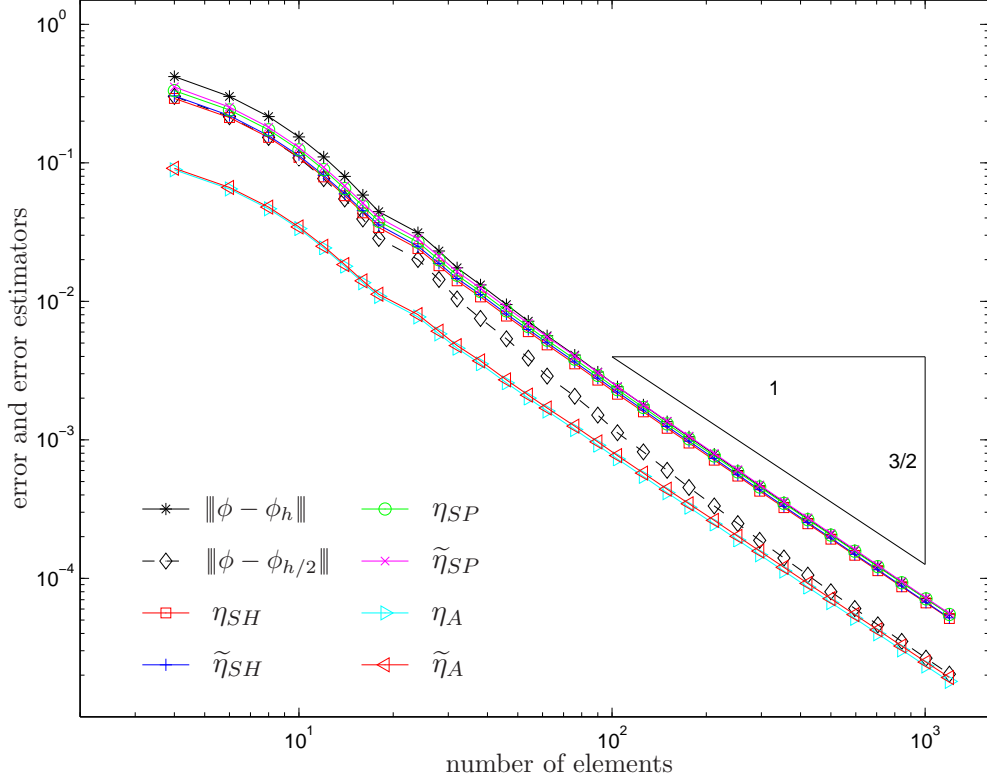


FIGURE 2. Errors $\|\phi - \phi_h\|$ and $\|\phi - \phi_{h/2}\|$ in Laplace Problem 6.3 as well as the six global error estimators for a sequence of μ_{SH} -adaptively generated meshes: We observe an optimal grading of the mesh in the sense that the optimal order $\mathcal{O}(N^{-3/2})$ of convergence is observed for the Galerkin error $\|\phi - \phi_h\|$. Moreover, we stress that $\|\phi - \phi_h\|$ is accurately estimated by η_{SH} , $\tilde{\eta}_{SH}$, η_{SP} , and $\tilde{\eta}_{SP}$, whereas η_A and $\tilde{\eta}_A$ are asymptotically accurate to estimate $\|\phi - \phi_{h/2}\|$.

The squared energy norm of the discrete solution ϕ_h reads $\|\phi_h\|^2 = \mathbf{A}\mathbf{x} \cdot \mathbf{x}$ with the Galerkin matrix \mathbf{A} and the coefficient vector \mathbf{x} corresponding to ϕ_h . In all experiments, the exact solution $\phi \in \tilde{H}^{-1/2}(\Gamma)$ is unknown. To compute the energy $\|\phi\|^2$, we therefore use Aitkin's Δ^2 -extrapolation as follows: For a sequence $\mathcal{T}_h^{(k)}$ of uniformly refined meshes, we compute the sequence of energies $E_k = \|\phi_h^{(k)}\|^2$, where $\phi_h^{(k)}$ denotes the discrete solution corresponding to the triangulation $\mathcal{T}_h^{(k)}$. Extrapolation of the sequence E_k then yields a good approximation of $\|\phi\|^2$.

In particular, this allows to compute the experimental saturation constants

$$q_{SH} := \|\phi - \phi_{h/2}\| / \|\phi - \phi_h\| \quad \text{and} \quad q_{SP} := \|\phi - \phi_h^{(1)}\| / \|\phi - \phi_h\|$$

as well as

$$q_A := \|\phi - \phi_h^{(1)}\| / \|\phi - \phi_{h/2}\| = q_{SP} / q_{SH}.$$

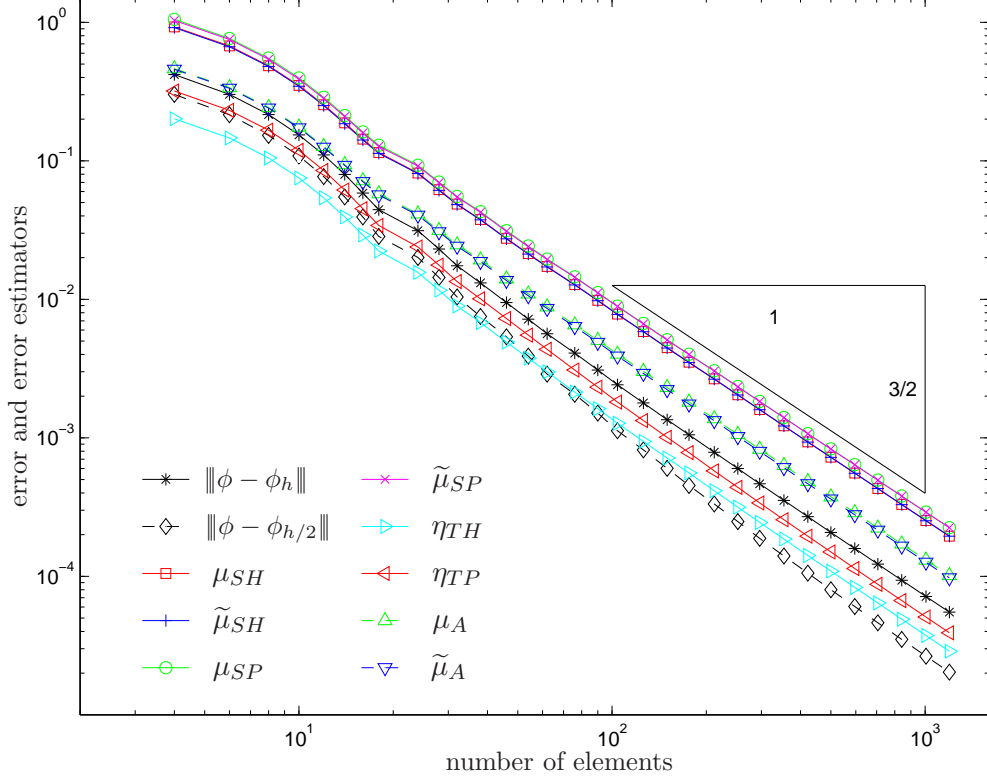


FIGURE 3. Errors $\|\phi - \phi_h\|$ and $\|\phi - \phi_{h/2}\|$ in Laplace Problem 6.3 as well as various local error estimators for a sequence of μ_{SH} -adaptively generated meshes: We observe an optimal grading of the mesh in the sense that the optimal order $\mathcal{O}(N^{-3/2})$ of convergence is observed for the Galerkin error $\|\phi - \phi_h\|$.

The computation of the constant λ_A from (5.4) leads to a generalized eigenvalue problem: Note that

$$\lambda_A^2 = \max_{\psi_h^{(1)} \in X_h^{(1)}} \frac{\|\psi_h^{(1)} - \mathbb{G}_{h/2}\psi_h^{(1)}\|^2}{\|\psi_h^{(1)}\|^2} = \max_{\psi_h^{(1)} \in X_h^{(1)}} \frac{\|\psi_h^{(1)}\|^2 - \|\mathbb{G}_{h/2}\psi_h^{(1)}\|^2}{\|\psi_h^{(1)}\|^2}$$

For $\mathcal{T}_h = \{T_1, \dots, T_N\}$, there holds $\dim X_h^{(1)} = \dim X_{h/2} = 2N$. Let $\{\phi_1, \dots, \phi_{2N}\}$ be a basis of $X_h^{(1)}$ and $\{\chi_1, \dots, \chi_{2N}\}$ be a basis of $X_{h/2}$. For arbitrary $\psi_h^{(1)} \in X_h^{(1)}$, we consider the basis representations

$$\psi_h^{(1)} = \sum_{k=1}^{2N} \mathbf{x}_k \phi_k \quad \text{as well as} \quad \mathbb{G}_{h/2}\psi_h^{(1)} = \sum_{k=1}^{2N} \mathbf{y}_k \chi_k$$

with coefficient vectors $\mathbf{x}, \mathbf{y} \in \mathbb{R}^{2N}$. We define the matrices $\mathbf{A}, \mathbf{B} \in \mathbb{R}_{\text{sym}}^{2N \times 2N}$ and $\mathbf{C} \in \mathbb{R}^{2N \times 2N}$

$$\mathbf{A}_{jk} := \langle \phi_k, \phi_j \rangle \quad \mathbf{B}_{jk} := \langle \chi_k, \chi_j \rangle \quad \mathbf{C}_{jk} := \langle \phi_k, \chi_j \rangle.$$

Clearly, \mathbf{A} and \mathbf{B} are positive definit, and there holds

$$\|\psi_h^{(1)}\|^2 = \mathbf{A}\mathbf{x} \cdot \mathbf{x} \quad \text{as well as} \quad \|\mathbb{G}_{h/2}\psi_h^{(1)}\|^2 = \mathbf{B}\mathbf{y} \cdot \mathbf{y}.$$

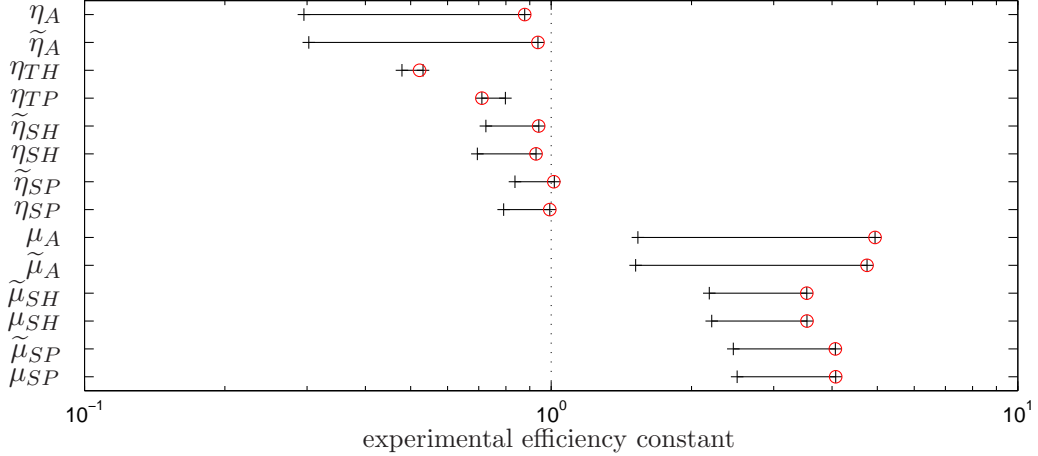


FIGURE 4. *Experimental efficiency constants C_{eff} of error estimators for μ_{SH} -adaptive mesh-refinement in Laplace Problem 6.3: Note that the intervals indicate the range of the efficiency constant C_{eff} , whereas the red circle indicates the precise value of C_{eff} in the final step of the adaptive computation. For the h - $h/2$ -based and p - $(p+1)$ -based error estimators we consider the ratio of error estimator and $\|\phi - \phi_h\|$, e.g., $C_{\text{eff}} = \eta_{SH} / \|\phi - \phi_h\|$. Since the averaging error estimators are expected to estimate $\|\phi - \phi_{h/2}\|$, we consider the ratio of estimator and $\|\phi - \phi_{h/2}\|$ instead, e.g., $C_{\text{eff}} = \eta_A / \|\phi - \phi_{h/2}\|$.*

Moreover, the coefficient vector \mathbf{y} is obtained by solving the linear system

$$\mathbf{B}\mathbf{y} = \mathbf{C}\mathbf{x}.$$

Plugging everything together, we thus obtain

$$\frac{\|\psi_h^{(1)}\|^2 - \|\mathbb{G}_{h/2}\psi_h^{(1)}\|^2}{\|\psi_h^{(1)}\|^2} = \frac{\mathbf{A}\mathbf{x} \cdot \mathbf{x} - \mathbf{B}\mathbf{y} \cdot \mathbf{y}}{\mathbf{A}\mathbf{x} \cdot \mathbf{x}} = \frac{(\mathbf{A} - \mathbf{C}^T\mathbf{B}^{-1}\mathbf{C})\mathbf{x} \cdot \mathbf{x}}{\mathbf{A}\mathbf{x} \cdot \mathbf{x}},$$

which results in the generalized Rayleigh quotient

$$\lambda_A^2 = \max_{\mathbf{x} \in \mathbb{R}^{2N}} \frac{\mathbf{M}\mathbf{x} \cdot \mathbf{x}}{\mathbf{A}\mathbf{x} \cdot \mathbf{x}}$$

with the positive semi-definit matrix $\mathbf{M} := \mathbf{A} - \mathbf{C}^T\mathbf{B}^{-1}\mathbf{C} \in \mathbb{R}_{\text{sym}}^{2N \times 2N}$. Therefore, λ_A^2 is the largest generalized eigenvalue $\mu > 0$ of the system $\mathbf{M}\mathbf{x} = \mu\mathbf{A}\mathbf{x}$. For the numerical experiments provided below, we computed λ_A^2 by use of the MATLAB function `eig`.

6.3. Laplace Problem. In our first experiment, we consider

$$(6.1) \quad V\phi = 1 \quad \text{on } \Gamma = (0, 1),$$

where V denotes the simple-layer potential (1.2) of the Laplace equation. Aitkin's Δ^2 -method yields $\|\phi\|^2 = 4.53236014183015$. The initial mesh consists of four intervals with uniform mesh-size 0.25. For uniform mesh-refinement, we experimentally observe a suboptimal order of convergence $\|\phi - \phi_h\| = \mathcal{O}(h^{1/2})$ which is far from being optimal. However, all proposed adaptive strategies recover the optimal order of convergence. To keep the presentation short, Figure 2–3 only show the numerical outcome in case of μ_{SH} -adaptive mesh-refinement: We use Algorithm 3.3 with refinement indicators $\mu_{SH,j} = h_j^{1/2}\|\phi_{h/2} - \phi_h\|_{L^2(T_j)}$ and marking parameter $\theta = 0.5$ to create a sequence of adaptively refined meshes. The computed values

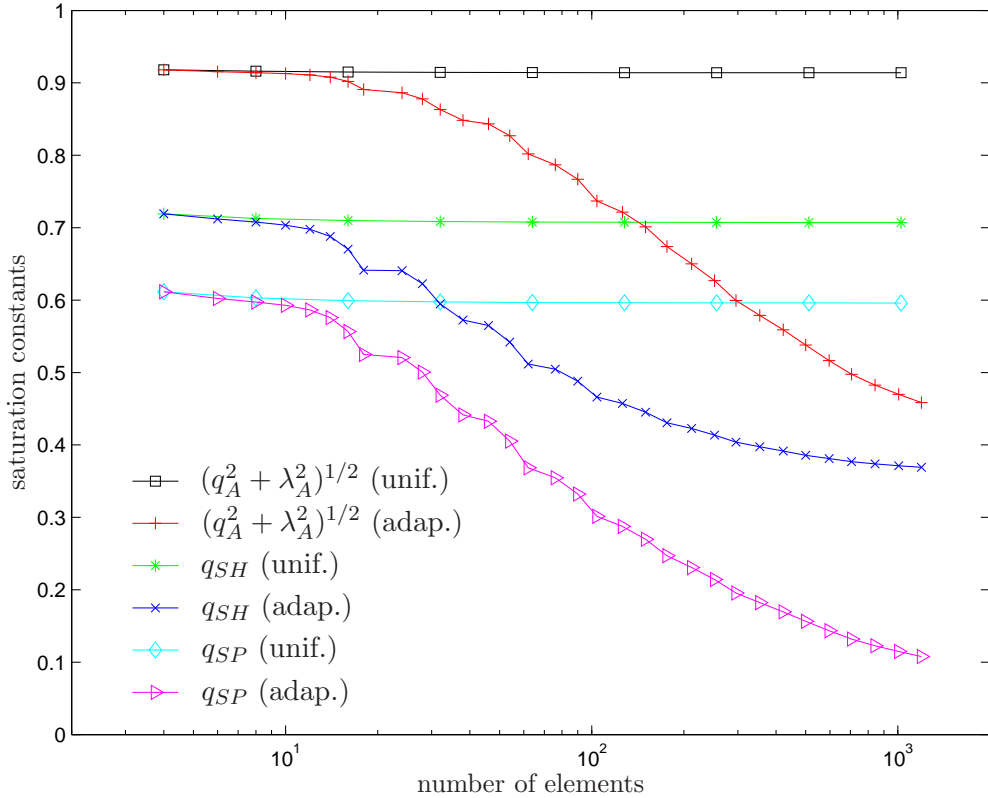


FIGURE 5. All experimental saturation constants in Laplace Problem 6.3 are uniformly bounded < 1 , which yields reliability of all error estimators. We stress that all constants appear to depend on the smoothness of the unknown solution ϕ in the sense that they are improved in case of μ_{SH} -adaptive mesh-refinement.

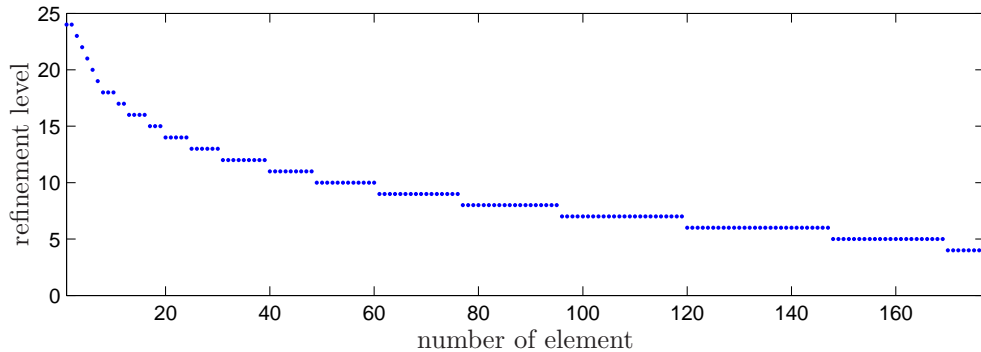


FIGURE 6. Adaptive mesh-refinement in Laplace Problem 6.3: The exact solution as well as the meshes appear to be symmetric with respect to the slit's midpoint, so that we only show the generated elements on the left half $(0, 1/2)$ of the slit. We consider an μ_{SH} -adaptively generated mesh with $N = 354$ elements after 24 steps of our adaptive algorithm. We number the elements from left to right. For each element T_j , we then plot its refinement level $1/(4h_j)$, i.e. the quotient of initial mesh-width $1/4$ and the element-width h_j , over the number j of the element.

of the Galerkin errors $\|\phi - \phi_h\|$ and $\|\phi - \phi_{h/2}\|$ as well as of all error estimators are plotted over the number N of elements. The logarithmic scaling of both axes yields that an algebraic

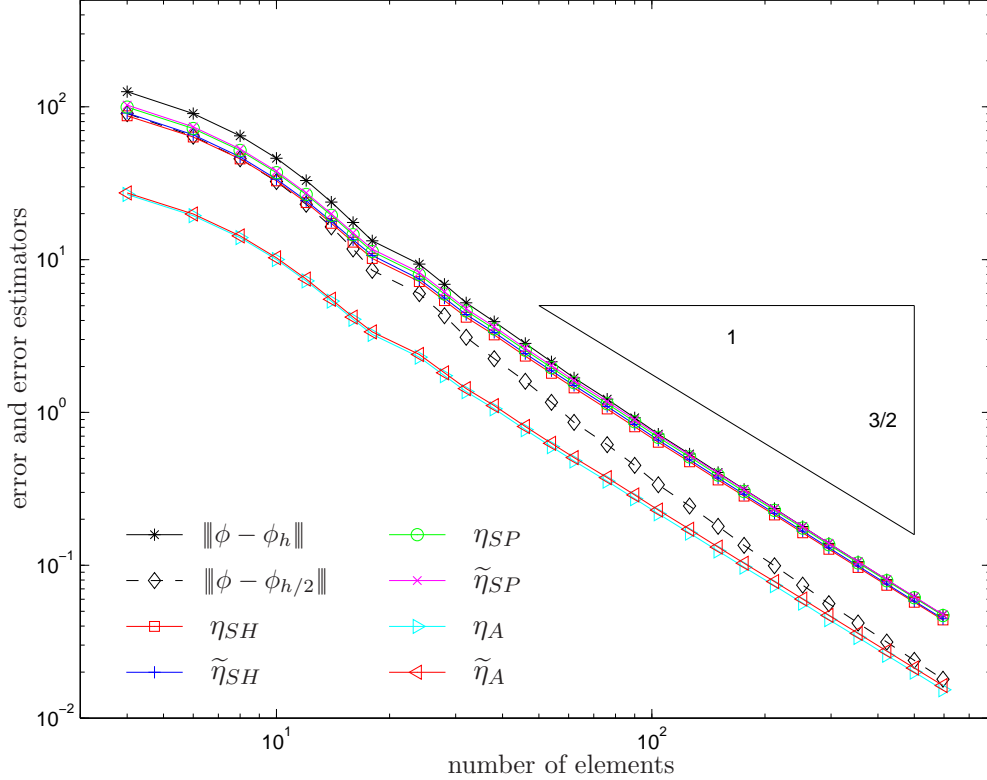


FIGURE 7. Galerkin errors as well as global error estimators in Lamé Problem 6.4: The μ_{SH} -adaptive mesh-refinements leads to the optimal order $\mathcal{O}(N^{-3/2})$ of convergence. Moreover, $\|\phi - \phi_h\|$ is accurately estimated by η_{SH} , $\tilde{\eta}_{SH}$, η_{SP} , and $\tilde{\eta}_{SP}$, whereas η_A and $\tilde{\eta}_A$ are asymptotically accurate estimators for $\|\phi - \phi_{h/2}\|$.

dependence $\mathcal{O}(N^{-\alpha})$ for some $\alpha > 0$ results in a straight line with slope $-\alpha$. Note that the experimentally observed slope $\alpha = 3/2$ corresponds to the optimal order of convergence. All curves appear to be parallel, which corresponds to the fact that all error estimators are observed to be reliable and efficient.

Moreover, Figure 2 shows that the energy norm based (and non-local) error estimators η_{SH} , $\tilde{\eta}_{SH}$, η_{SP} , and $\tilde{\eta}_{SP}$ are very accurate error estimators for $\|\phi - \phi_h\|$. The averaging-based error estimators η_A and $\tilde{\eta}_A$ appear to be asymptotically accurate for the estimation of the improved Galerkin error $\|\phi - \phi_{h/2}\|$.

Figure 4 visualizes the experimental efficiency constants. For h - $h/2$ -based and p - $(p+1)$ -based error estimators, e.g. η_{SH} , we visualize the range of $C_{\text{eff}} = \eta_{SH}/\|\phi - \phi_h\|$ as well as the precise value in the final step of our adaptive computation. For the averaging-based error estimators, e.g. η_A , which are expected to estimate the improved Galerkin error $\|\phi - \phi_{h/2}\|$, we visualize $C_{\text{eff}} = \eta_A/\|\phi - \phi_{h/2}\|$ instead. For all error estimators, the experimental efficiency constant C_{eff} varies in a range between $3/10$ and 5 . For the error estimators η_{SH} , $\tilde{\eta}_{SH}$, η_{SP} , and $\tilde{\eta}_{SP}$, we observe that C_{eff} is improved by adaptive mesh-refinement and seems to converge to 1 , which corresponds to asymptotically exact error estimation. As expected, the best coincidence of error $\|\phi - \phi_h\|$ and error estimator is observed in case of η_{SP} .

Whereas efficiency of the introduced error estimators is predicted by theory, the reliability depends on certain saturation assumptions, namely $q_{SH} < 1$ in case of h - $h/2$ -based error

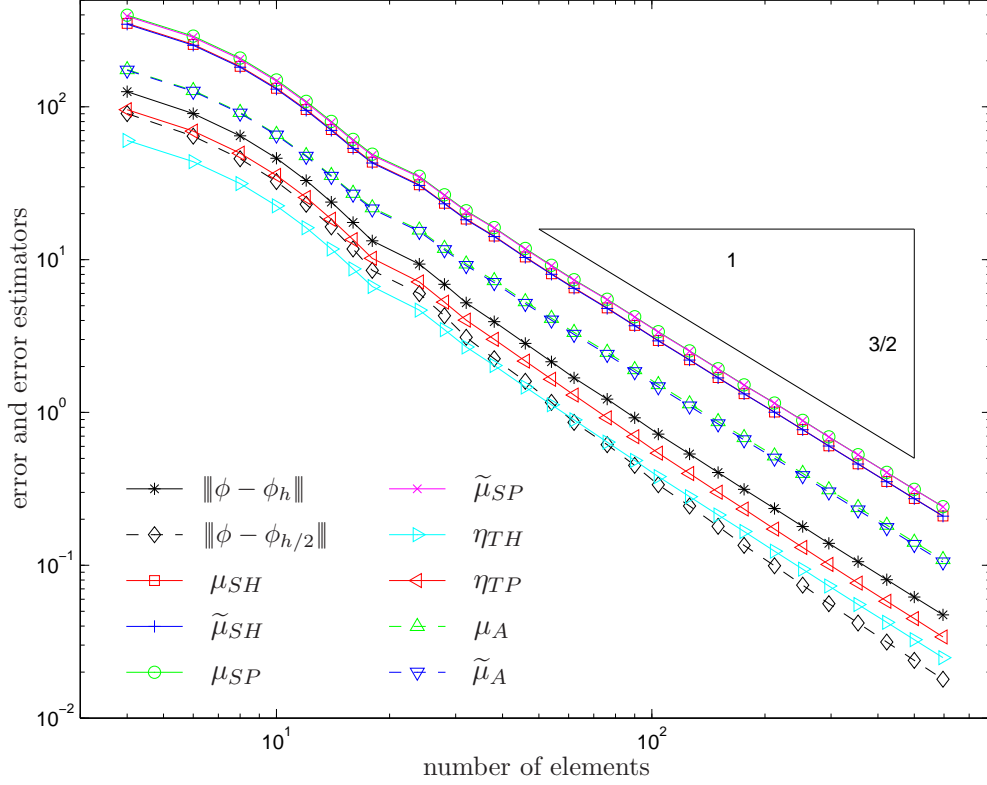


FIGURE 8. Galerkin errors and various local error estimators in Lamé Problem 6.4 for μ_{SH} -adaptive mesh-refinement.

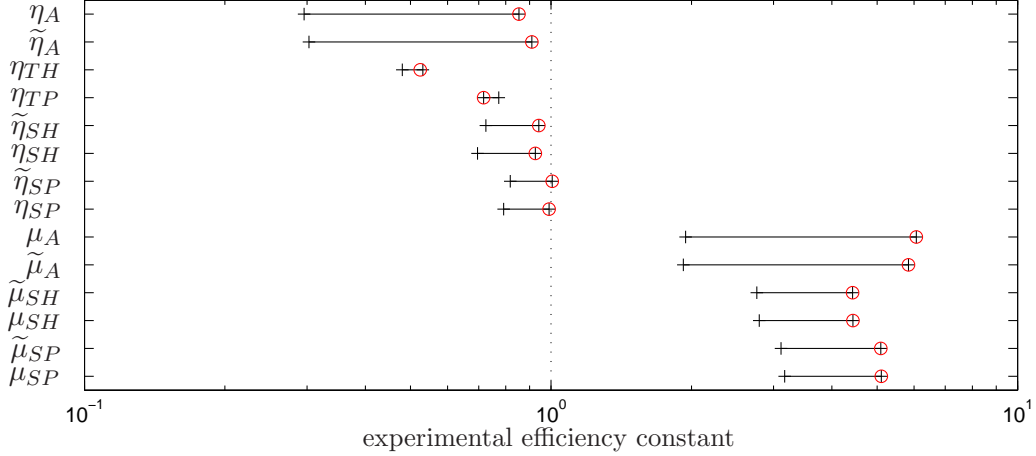


FIGURE 9. Experimental efficiency constants C_{eff} for μ_{SH} -adaptive mesh-refinement in Lamé Problem 6.4: The intervals indicate the range C_{eff} , whereas the red circle indicates the precise value of C_{eff} in the final step of the adaptive computation. For the h - $h/2$ -based and p - $(p+1)$ -based error estimators, we compute C_{eff} with respect to $\|\phi - \phi_h\|$, e.g., $C_{\text{eff}} = \eta_{SH}/\|\phi - \phi_h\|$. For the averaging error estimators, we consider the ratio of estimator and $\|\phi - \phi_{h/2}\|$ instead, e.g., $C_{\text{eff}} = \eta_A/\|\phi - \phi_{h/2}\|$.

estimation, $q_{SP} < 1$ in case of p - $(p+1)$ -based error estimation, and $q_A^2 + \lambda_A^2 < 1$ in case of averaging-based error estimation, respectively. Figure 5 plots these three constants over the

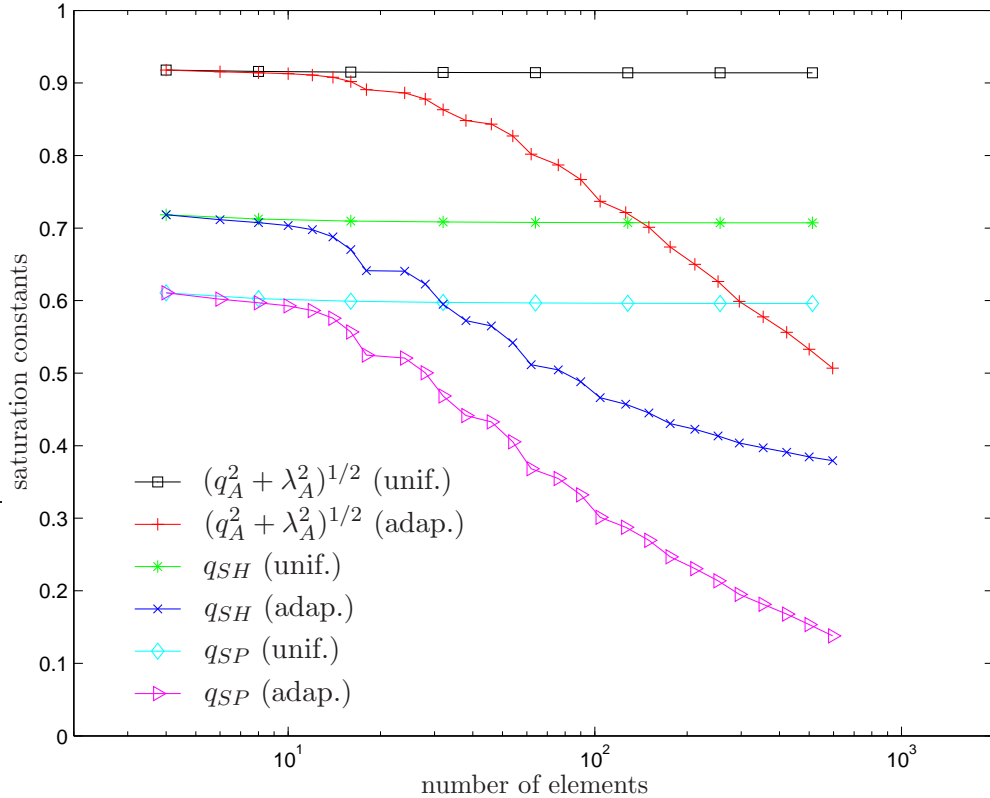


FIGURE 10. All experimental saturation constants in Lamé Problem 6.4 are uniformly bounded < 1 . We expect dependence on the smoothness of the unknown solution ϕ in the sense that the constants are improved in case of μ_{SH} -adaptive mesh-refinement.

number of elements in case of uniform and adaptive mesh-refinement. In any case, we observe that all constants are uniformly bounded away from 1. This empirically proves reliability of the error estimators. We stress that all constants appear to depend on the smoothness of the unknown solution ϕ in the sense that they are improved in case of the adaptive mesh-refining strategy. Moreover, this explains that the observation that the accuracy of the error estimation, e.g. for η_{SH} , is improved by adaptive mesh-refinement.

The computed discrete solutions as well as the adaptively generated meshes appear to be symmetric with respect to the slit's midpoint $(1/2, 0)$. Figure 6 visualizes the refinement for an adaptively generated mesh with $N = 354$ elements after 24 steps of our adaptive algorithm. We observe a very strong refinement towards the left and right endpoints of the slit.

6.4. Lamé problem. The exterior Navier-Lamé problem consists of the equation

$$(6.2) \quad -\Delta^* u := -\mu \Delta u - (\lambda + \mu) \operatorname{grad} \operatorname{div} u = 0 \quad \text{in } \mathbb{R}^2 \setminus \Gamma, \quad \Gamma = (0, 1)$$

and a radiation condition of the form [10, 11]

$$D^\alpha(u - a)(x) = \mathcal{O}(|x|^{-1-\alpha}) \quad \text{for } |x| \rightarrow \infty \quad \text{and} \quad \alpha = 0, 1,$$

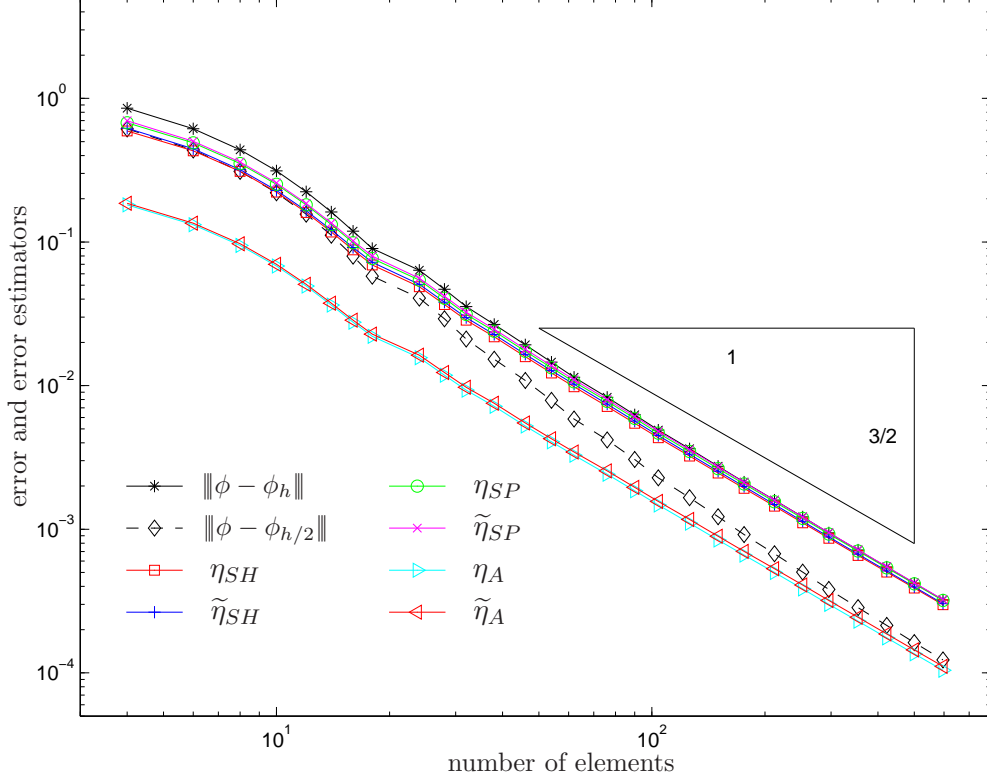


FIGURE 11. Galerkin errors and global error estimators for Stokes Problem 6.5 and μ_{SH} -adaptive mesh-refinement: We observe the optimal order $\mathcal{O}(N^{-3/2})$ of convergence. Moreover, $\|\phi - \phi_h\|$ is accurately estimated by η_{SH} , $\tilde{\eta}_{SH}$, η_{SP} , and $\tilde{\eta}_{SP}$, whereas η_A and $\tilde{\eta}_A$ are asymptotically accurate to estimate $\|\phi - \phi_{h/2}\|$.

where D^1 denotes the Jacobian and where $a \in \mathbb{R}^2$ is a given constant vector. The conormal derivative related to the Lamé operator Δ^* reads

$$T(u) := 2\mu\partial_n u + \lambda n \operatorname{div} u + \mu n \times \operatorname{curl} u$$

with the normal derivative ∂_n . The fundamental solution $E(x, y)$ of the Lamé operator, called Kelvin-matrix, is given by

$$E(x, y) = \frac{\lambda + 3\mu}{4\pi\mu(\lambda + 2\mu)} \left\{ \log \frac{1}{|x - y|} \cdot \mathbf{I} + \frac{\lambda + \mu}{\lambda + 3\mu} \frac{(x - y)(x - y)^T}{|x - y|^2} \right\},$$

where \mathbf{I} is the 2×2 unit matrix [13]. Since E is analytic in $\mathbb{R}^2 \times \mathbb{R}^2$ without the diagonal we may define its traction

$$T(x, y) := T_y(E(x, y))^T, \quad x \neq y.$$

As it is derived, e.g., in [10, 11, 13], there holds the Betti representation formula for $x \in \Omega$

$$(6.3) \quad u(x) = \langle T(x, \cdot), v \rangle - \langle E(x, \cdot), \phi \rangle + a$$

for all $u \in \{w \in (H_{loc}^1(\Omega))^2 : \text{there exists a constant } a \text{ s.t. } w \text{ satisfies (6.2) and (6.3)}\}$ with $v = u|_\Gamma$, $\phi = T(u)|_\Gamma$. The second term defines the simple-layer potential

$$(V\phi)(x) = \langle E(x, \cdot), \phi \rangle \quad (x \in \Gamma).$$

for the Lamé operator. For properties of the simple-layer potential we refer to [5, 6].

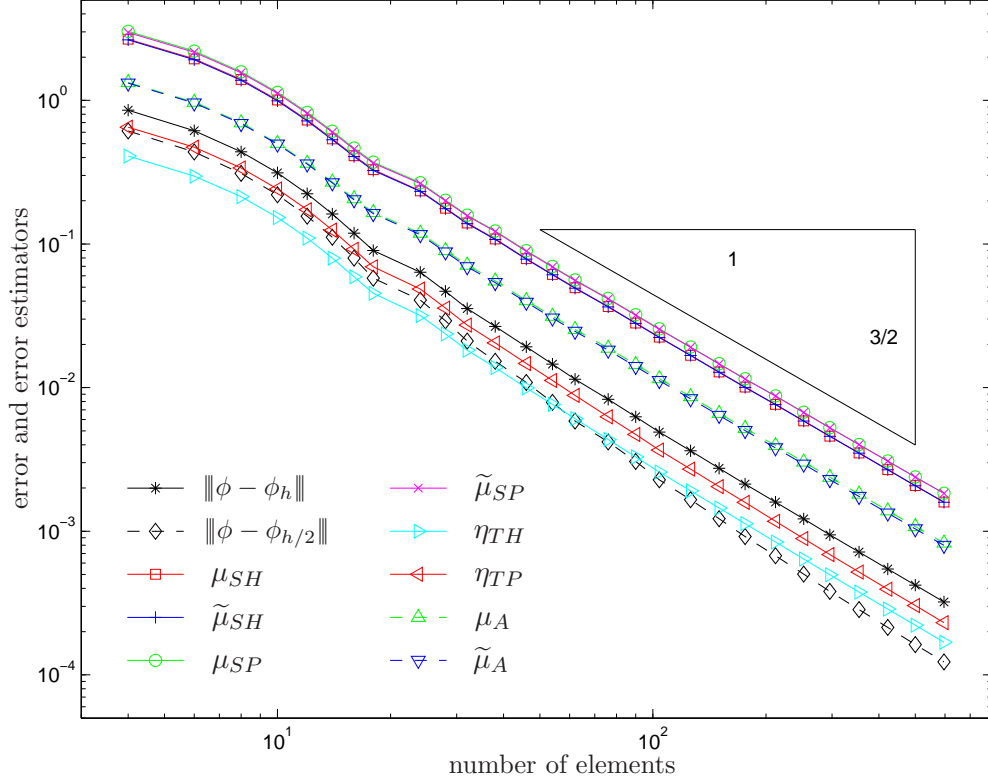


FIGURE 12. Galerkin errors and further error estimators in Stokes Problem 6.5 for μ_{SH} -adaptive mesh-refinement.

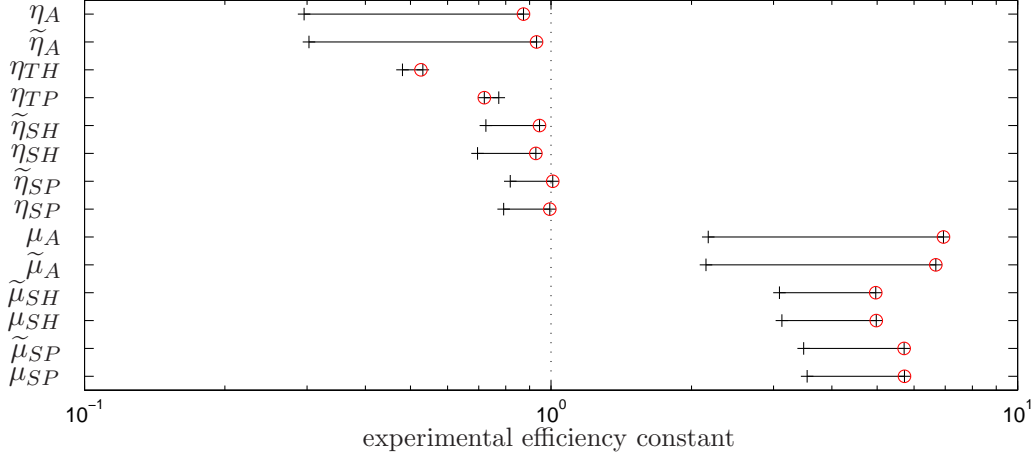


FIGURE 13. Experimental efficiency constants C_{eff} for μ_{SH} -adaptive mesh-refinement in Stokes Problem 6.5: The intervals indicate the range C_{eff} , whereas the red circles indicate the precise values of C_{eff} in the final steps of the adaptive computation. For the h - $h/2$ -based and p - $(p+1)$ -based error estimators, we compute C_{eff} with respect to $\|\phi - \phi_h\|$, e.g., $C_{\text{eff}} = \eta_{SH}/\|\phi - \phi_h\|$. For the averaging error estimators, we consider the ratio of estimator and $\|\phi - \phi_{h/2}\|$ instead, e.g., $C_{\text{eff}} = \eta_A/\|\phi - \phi_{h/2}\|$.

For the numerical experiment, we consider an infinite elastic plane of steel ($E = 10^5 [N/mm^2]$, $\nu = 1/3$) with a crack at $\Gamma = (0, 1)$. The Lamé coefficients are given by the relations

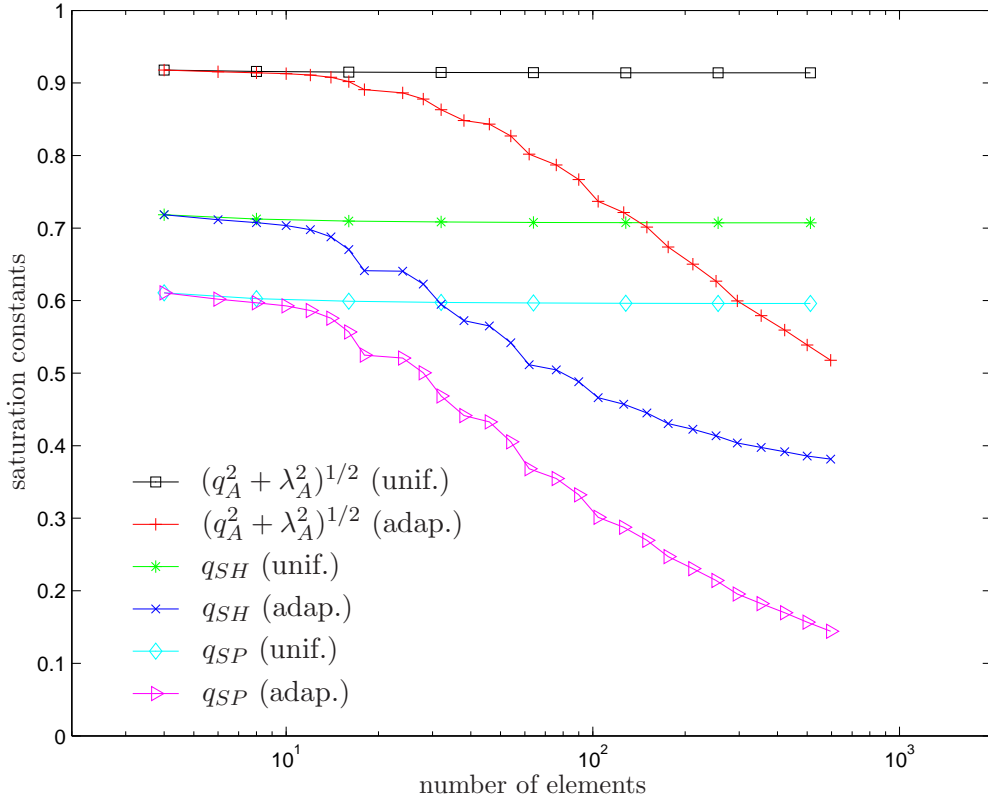


FIGURE 14. All experimental saturation constants in Stokes Problem 6.5 are uniformly bounded < 1 and improved for μ_{SH} -adaptive mesh-refinement.

$\lambda = \frac{E\nu}{(1-2\nu)(1+\nu)} = 75.000$ and $\mu = \frac{E}{2(1+\nu)} = 37.500$. We aim to approximate the exact solution $\phi \in (\tilde{H}^{-1/2}(\Gamma))^2$ of

$$V\phi = (1, 1)^\top \quad \text{on } \Gamma$$

and stress that the exact solution is unknown. Extrapolation, however, provides the squared energy $\|\phi\|^2 = 461737.806798923$.

Note that the ellipticity and continuity of the simple-layer potential V strongly depend on the Lamé coefficient μ . This results in a relatively small quotient of energy norm $\|\cdot\|$ and weighted L^2 -norm $\|h^{1/2}(\cdot)\|_{L^2(\Gamma)}$. As in [2], we therefore scale the L^2 -norm based error estimators by a factor $1/\sqrt{\mu}$, e.g.,

$$(6.4) \quad \tilde{\mu}_A := \frac{1}{\sqrt{\mu}} \|h^{1/2}(\phi_{h/2} - \Pi_h^{(1)}\phi_{h/2})\|_{L^2(\Gamma)}.$$

Figure 8 gives empirical evidence that this is the right scaling in the sense that it leads to almost the same results as for the Laplace Problem 6.3.

For the numerical computations, we used an initial mesh consisting of four equally sized intervals. As for the Laplace Problem 6.3, uniform mesh-refinement leads to a suboptimal order of convergence $\|\phi - \phi_h\| \approx \mathcal{O}(N^{-1/2})$. Instead, all proposed adaptive strategies show the optimal convergence rate $\mathcal{O}(N^{-3/2})$. The outcome of an μ_{SH} -adaptive computation is visualized in Figure 7–10. For more details about the figures, the reader is referred to the corresponding descriptions for the Laplace Problem 6.3.

6.5. Stokes problem. The exterior Stokes problem reads

$$\left. \begin{aligned} \operatorname{div} (2\mu\varepsilon(u) - p \cdot \mathbf{I}) &= 0 \\ \operatorname{div} u &= 0 \end{aligned} \right\} \quad \text{in } \mathbb{R}^2 \setminus (0, 1)$$

with the symmetric Green tensor $\varepsilon(\cdot) := (\nabla + \nabla^\top)/2$ and a radiation condition

$$u(x) = O(1) \quad (|x| \rightarrow \infty),$$

cf. [10, 11]. According to [12], the simple-layer potential V for the Stokes operator is defined by

$$(V\phi)(x) := \langle E(x, \cdot), \phi \rangle \quad (x \in \Gamma),$$

where

$$E(x, y) = \frac{1}{4\pi\mu} \left\{ \log \frac{1}{|x-y|} \cdot \mathbf{I} + \frac{(x-y)(x-y)^\top}{|x-y|^2} \right\},$$

In the following we consider the problem: Find $\phi \in (\tilde{H}^{-1/2}(\Gamma))^2$ s.t.

$$V\phi = (1, 1)^\top \quad \text{on } \Gamma = (0, 1).$$

The viscosity is chosen $\mu = 1.57 \text{ [Ns/m}^2\text{]}$, which corresponds to glycerin. For this setting, the extrapolated squared energy reads $\|\phi\|^2 = 22.0694024958539$.

The outcome of an μ_{SH} -adaptive computation is visualized in Figure 11–14. As for the Lamé Problem 6.4, we scale the L^2 -norm based error estimators by $1/\sqrt{\mu}$, cf. (6.4).

7. CONCLUSION

In this paper, we studied three classes of a posteriori error estimators for the Galerkin boundary element method. This includes error estimators derived from space enrichment, e.g., the h - $h/2$ -based error estimators introduced by FERRAZ-LEITE and PRAETORIUS [8], the two-level error estimator introduced by MUND, STEPHAN, and WEISSE [15], and the averaging estimators introduced by CARSTENSEN and PRAETORIUS [3]. Throughout, we focused on the lowest-order \mathcal{P}^0 -Galerkin scheme for $\tilde{H}^{-1/2}$ -elliptic integral operators. An overview on the studied error estimators is given in Section 6.1 above. All of these estimators can be covered within one analytical framework which is essentially based on a local inverse estimate and a local first-order approximation estimate for the $\tilde{H}^{-1/2}$ -norm. The analysis therefore applies for all elliptic pseudodifferential operators $A : \tilde{H}^{-1/2} \rightarrow H^{1/2}$ of negative order $\alpha = -1$.

7.1. Analytical Results. First, the numerical analysis of the pioneering work [15] is restricted to the case of uniform mesh-refinement. However, the numerical experiments of [15] indicated that the two-level error estimation technique is even capable to steer an adaptive anisotropic mesh-refinement in 3D. One aim of this paper was the generalization of the analysis of [15] to the case of adaptively generated meshes. Our proof justifies the numerical results of [15] for the 2D Galerkin BEM. In particular, our analysis is optimal in the sense that, besides the K-mesh property, there is almost no restriction on the adaptive meshes used.

Second, the averaging error estimators of [3] are so far only proven to be reliable and efficient under rather strong assumptions, which are discussed above. It came to a surprise of us that the averaging error estimators are equivalent to the h - $h/2$ -error estimators as well as to the two-level error estimator of [15]. In fact, we prove that all error estimators are

equivalent. In particular, we thus obtain that all of the error estimators are always efficient, whereas reliability holds under the saturation assumption.

7.2. Numerical Results. Besides the well studied simple-layer potential of the Laplace problem, cf. e.g. [15, 3, 4, 8], we considered the simple-layer potentials of the Lamé and the Stokes problem. The conclusions in the three examples are analogous and can be described as follows. The h -adaptive BEM refines the mesh towards the singularity. Note carefully, that only the endpoints are singular points. So far the meshes indicate that the h -adaptive scheme mimics a geometric mesh grading which is regarded as an optimal strategy.

The plots in Figure 2, 3, 7, 8, 11, and 12 represent the relative errors in the energy norm as a function of degrees of freedom for various experiments connected by straight lines. Note the logarithmic scaling on both axes so that an algebraic convergence results in a straight line with a slope which is the experimental convergence rate. For uniform mesh-refinement, one observes convergence rates which are poor according to the singularity (see [16] for a proof of that). This proves numerically, that our h -adaptive BEM is of optimal convergence rate and hence a powerful tool in the efficient treatment of integral equations of the first kind.

Finally, the error estimation of the global error estimators is very accurate in the sense that the values of, e.g., the h - $h/2$ -error estimator η_H and the corresponding Galerkin error $\|\phi - \phi_h\|$ almost coincide. To keep the implementational overhead as small as possible and according to Remark 3, we therefore propose to use the local contributions of the two-level error estimator η_{TH} to steer the adaptive mesh-refinement and to use η_H to estimate the (unknown) Galerkin error.

7.3. Extensions and Future Work. The numerical experiments of Section 6 show that the involved saturation assumptions are satisfied in praxis. Thus, it has to be a mayor goal of our future research to prove the saturation assumption mathematically.

Our analytical results can be extended in the following ways: First, local inverse estimates and local first-approximation approximation results are even available for the $\tilde{H}^{1/2}$ -norm. Therefore, analogous results can be achieved for the hypersingular integral operators $A : \tilde{H}^{1/2} \rightarrow H^{-1/2}$ in 2D Galerkin BEM. Details are postponed to a forthcoming paper.

An extension of the results to the 3D Galerkin BEM is, so far, only possible for shape-regular triangulations. The experiments of [15, 8] however indicate that all error estimators perform well even in case of anisotropic mesh-refinement.

REFERENCES

- [1] C. CARSTENSEN, S. A. FUNKEN, E. P. STEPHAN: *A Posteriori Error Estimates for h - p -Boundary Element Methods*, Appl. Ana. 61 (1996), 233–253.
- [2] C. CARSTENSEN, S. A. FUNKEN: *Averaging Technique for FE A Posteriori Error Control in Elasticity. Part II: λ -Independent Estimates*, Comp. Meth. Appl. Mech. Engrg. 190 (2001), 4663–4675.
- [3] C. CARSTENSEN, D. PRAETORIUS: *Averaging Techniques for the Effective Numerical Solution of Symm’s Integral Equation of the First Kind*, SIAM J. Sci. Comp. 27 (2006), 1226–1260.
- [4] C. CARSTENSEN, D. PRAETORIUS: *Averaging Techniques for A Posteriori Error Control in Finite Element and Boundary Element Analysis*, Computational Mechanics 29 (2007), 29–59.
- [5] M. COSTABEL: *Boundary Integral Operators on Lipschitz Domains: Elementary Results*, SIAM J. Math. Anal. 19 (1988), 613–626.

- [6] M. COSTABEL, E.P. STEPHAN: *Coupling of Finite and Boundary Element Methods for an Elastoplastic Interface Problem*, SIAM J. Numer. Anal. 27 (1990), 1212–1226.
- [7] W. DOERFLER, R. NOCHETTO: *Small Data Oscillation Implies the Saturation Assumption*, Numer. Math. 91 (2002), 1–12.
- [8] S. FERRAZ-LEITE, D. PRAETORIUS: *Simple A Posteriori Error Estimators for the h-Version of the Boundary Element Method*, submitted 2007.
- [9] I.G. GRAHAM, W. HACKBUSCH, S.A. SAUTER: *Finite Elements on Degenerate Meshes: Inverse-Type Inequalities and Applications*, IMA J. Numer. Anal. 25 (2005), 379–407.
- [10] G.C. HSIAO, P. KOPP, W.L. WENDLAND: *Some Applications of a Galerkin-Collocation Method for Boundary Integral Equations of the First Kind*, Math. Methods Appl. Sci. 6 (1984) 280–325.
- [11] G.C. HSIAO, E.P. STEPHAN, W.L. WENDLAND: *On the Dirichlet Problem in Elasticity for a Domain Exterior to an Arc*, J. CAM 34 (1991) 1–19.
- [12] G.C. HSIAO, R. KRESS: *On an Integral Equation for the Two-Dimensional Exterior Stokes Problem*, Appl. Numer. Math. 1 (1985) 77–93.
- [13] G.C. HSIAO, W.L. WENDLAND: *On a Boundary Integral Method for some Exterior Problems in Elasticity*, Proc. Tbilisi Univ. 257 (1985) 31–60.
- [14] M. MAISCHAK: *The Analytical Computation of the Galerkin Elements for the Laplace, Lamé and Helmholtz Equation in 2D BEM*, Preprint (1999), Institut für Angewandte Mathematik, Universität Hannover.
- [15] P. MUND, E.P. STEPHAN, J. WEISSE: *Two-Level Methods for the Single Layer Potential in \mathbb{R}^3* , Computing 60 (1998), 243–266.
- [16] E.P. STEPHAN, M. SURI: *The hp-version of the Boundary Element Method on polygonal domains with quasi uniform meshes*, Math. Model. Num. Anal. 25 (1991), 783–807.

INSTITUTE FOR ANALYSIS AND SCIENTIFIC COMPUTING, VIENNA UNIVERSITY OF TECHNOLOGY, WIEDNER HAUPTSTRASSE 8-10, A-1040 WIEN, AUSTRIA
E-mail address: Dirk.Praetorius@tuwien.ac.at

INSTITUTE FOR NUMERICAL MATHEMATICS, UNIVERSITY OF ULM, HELMHOLTZSTRASSE 18, D-89069 ULM, GERMANY
E-mail address: {Stefan.Funken, Christoph.Erath}@uni-ulm.de